NASA/CR—2003-212540

Measurement of Turbulent Pressure and Temperature Fluctuations in a Gas Turbine Combustor

Andrea Passaro
Centrospazio–CPR, Pisa, Italy

John E. LaGraff
Syracuse University, Syracuse, New York

Martin L.G. Oldfield
University of Oxford, Oxford, United Kingdom

Leonardo Biagioni
Centrospazio – CPR, Pisa, Italy

Roger W. Moss
University of Newcastle upon Tyne, Newcastle upon Tyne, United Kingdom

Ryan T. Battelle
Syracuse University, Syracuse, New York

September 2003

The NASA STI Program Office . . . in Profile

Since its founding, NASA has been dedicated to the advancement of aeronautics and space science. The NASA Scientific and Technical Information (STI) Program Office plays a key part in helping NASA maintain this important role.

The NASA STI Program Office is operated by Langley Research Center, the Lead Center for NASA's scientific and technical information. The NASA STI Program Office provides access to the NASA STI Database, the largest collection of aeronautical and space science STI in the world. The Program Office is also NASA's institutional mechanism for disseminating the results of its research and development activities. These results are published by NASA in the NASA STI Report Series, which includes the following report types:

- TECHNICAL PUBLICATION. Reports of completed research or a major significant phase of research that present the results of NASA programs and include extensive data or theoretical analysis. Includes compilations of significant scientific and technical data and information deemed to be of continuing reference value. NASA's counterpart of peer-reviewed formal professional papers but has less stringent limitations on manuscript length and extent of graphic presentations.

- TECHNICAL MEMORANDUM. Scientific and technical findings that are preliminary or of specialized interest, e.g., quick release reports, working papers, and bibliographies that contain minimal annotation. Does not contain extensive analysis.

- CONTRACTOR REPORT. Scientific and technical findings by NASA-sponsored contractors and grantees.

- CONFERENCE PUBLICATION. Collected papers from scientific and technical conferences, symposia, seminars, or other meetings sponsored or cosponsored by NASA.

- SPECIAL PUBLICATION. Scientific, technical, or historical information from NASA programs, projects, and missions, often concerned with subjects having substantial public interest.

- TECHNICAL TRANSLATION. English-language translations of foreign scientific and technical material pertinent to NASA's mission.

Specialized services that complement the STI Program Office's diverse offerings include creating custom thesauri, building customized databases, organizing and publishing research results . . . even providing videos.

For more information about the NASA STI Program Office, see the following:

- Access the NASA STI Program Home Page at ***http://www.sti.nasa.gov***

- E-mail your question via the Internet to help@sti.nasa.gov

- Fax your question to the NASA Access Help Desk at 301–621–0134

- Telephone the NASA Access Help Desk at 301–621–0390

- Write to:
  NASA Access Help Desk
  NASA Center for AeroSpace Information
  7121 Standard Drive
  Hanover, MD 21076

NASA/CR—2003-212540

Measurement of Turbulent Pressure and Temperature Fluctuations in a Gas Turbine Combustor

Andrea Passaro
Centrospazio–CPR, Pisa, Italy

John E. LaGraff
Syracuse University, Syracuse, New York

Martin L.G. Oldfield
University of Oxford, Oxford, United Kingdom

Leonardo Biagioni
Centrospazio–CPR, Pisa, Italy

Roger W. Moss
University of Newcastle upon Tyne, Newcastle upon Tyne, United Kingdom

Ryan T. Battelle
Syracuse University, Syracuse, New York

Prepared under Grant NAG3–2419

National Aeronautics and
Space Administration

Glenn Research Center

September 2003

Acknowledgments

The authors of this work have been actively supported by Professor Luca d'Agostino, Università degli Studi di Pisa, whose help is gratefully acknowledged. The authors also wish to acknowledge the help provided by Simona Torre and Nicolas Pondicq-Cassou while working at Syracuse University, to complete their final year thesis work for Università degli Studi di Pisa and ENSICA Toulouse respectively, and the help from Trevor Godfrey and Laleah Carscallen at the University of Oxford. Finally the authors wish to thank ENEL personnel and in particular Mr. Giancarlo Benelli, Mr. Massimo Balestri, and Mr. Valerio Cinti, for the support offered during the tests in Sesta. This work was supported by NASA Grant NAG3–2419 with Dr. Louis Povinelli as technical supervisor, and through the framework cultural agreement between Syracuse University and Università degli Studi di Pisa.

Available from

NASA Center for Aerospace Information
7121 Standard Drive
Hanover, MD 21076

National Technical Information Service
5285 Port Royal Road
Springfield, VA 22100

Available electronically at http://gltrs.grc.nasa.gov

Measurement of Turbulent Pressure and Temperature Fluctuations in a Gas Turbine Combustor

Andrea Passaro
Centrospazio–CPR
Pisa, Italy

John E. LaGraff
Syracuse University
Syracuse, New York

Martin L.G. Oldfield
University of Oxford
Oxford, United Kingdom

Leonardo Biagioni
Centrospazio–CPR
Pisa, Italy

Roger W. Moss
University of Newcastle upon Tyne
Newcastle upon Tyne, United Kingdom

Ryan T. Battelle
Syracuse University
Syracuse, New York

ABSTRACT

The proper characterization of unsteady fluctuations in the outflow from gas turbine combustors during actual operation is greatly relevant to industrial equipment designers and manufacturers, because of the direct impact on turbine blade heat transfer and hence on the efficiency, life and safety of turbines. This is especially the case for lean-flame combustors operating near the stability limits to reduce pollutant emissions and for the higher pressure, higher temperature applications envisaged in the future. The turbulence level at the combustor exit directly affects the heat transfer rate to the nozzle guide vanes and to the downstream turbine blades, with crucial effects on the cooling requirements of these components. Unfortunately, because of the limitations of existing experimental techniques and of the severe conditions (1600 K, 20 atmospheres, or more) in this flow region, little (if any) experimental information on the flow unsteady properties is available on combustors operating near their design conditions.

The present research concerns the development of high-frequency pressure and temperature probes and related instrumentation capable of performing spectral characterization of unsteady pressure and temperature fluctuations over the 0.05–20 kHz range, at the exit of a gas turbine combustor operating at conditions close to nominal ones for large power generation turbomachinery. The probes used a transient technique pioneered at Oxford University; in order to withstand exposure to the harsh environment the probes were fitted on a rapid injection and cooling system jointly developed by Centrospazio-CPR and Syracuse University. The experimental runs were performed on a large industrial test rig being operated by ENEL Produzione.

The achieved results clearly show the satisfactory performance provided by this diagnostic tool, even though the poor location of the injection port prevented the tests from yielding more insight of the core flow turbulence characteristics. The pressure and temperature probes survived several dozen injections in the combustor hot jet, while consistently providing the intended high frequency performance. The apparatus was kept connected to the combustor during long duration firings, operating as an unobtrusive, self contained, piggy-back experiment: high frequency flow samplings were remotely recorded at selected moments corresponding to different combustor operating conditions.

1. Introduction

The development of high performance, efficient, reliable and environmentally compatible gas turbine engines crucially depends on the optimisation of the combustion process and on the attainment of high gas temperatures at the turbine inlet, which represents the most stringent thermodynamic limitation of current designs [Kerrebrock, 1992]. In this respect, the turbulence level and spectrum of the flow entering the turbine are extremely important parameters since they provide direct information on the operation and effectiveness of the combustor and, together with the average gas temperature, determine the heat transfer to the turbine blades, with obvious impacts on their equilibrium temperature and cooling requirements.

Knowledge of the turbulent fluctuation patterns in the exit flow from a combustor enables the designer to evaluate the success of the mixing processes, especially when considering the dilution flows toward the outlet end of the combustor. The unsteadiness of the gas temperature, in particular, is usually associated with lower combustion efficiencies than estimated based on the average flow conditions. It also results in higher pollutant formation (especially NO_x) and thermal damage to the turbine blades, both of which are strongly non-linear functions of the gas temperature. Low frequency fluctuations can be spectrally analysed for periodic signals symptomatic of potentially destructive acoustic resonance and flow instabilities, especially in lean-flame combustors operating near the stability limits to reduce pollutant emissions and in the higher pressure, higher temperature applications envisaged in the future.

2. Probe theory

Measurements of unsteady components of velocity, pressure and temperature in gas turbine combustors have traditionally been accomplished using two different types of devices: immersion type instruments and optical instruments. Optical methods for temperature measurement [Dyne and Penner, 1953; Fagan and Fleeter, 1994; Klavuhn *et al*., 1994] have the unique advantage of being non-intrusive, but usually involve averages over the field of view and are therefore incapable of yielding spatially and time resolved measurements of non-uniform unsteady flows. Usually, each method is capable of monitoring only a limited number of thermally excited states in a combustion gas mixture. Although this information can be valuable in the study of reaction processes, it often proves impossible to eliminate all instances of non-equilibrium excitation in order to obtain the thermodynamic temperature, as usually required [Anderson and Eckbreth, 1992; Gulati, 1994; Gulati and Warren, 1994]. Measurements exceeding the adiabatic flame temperature have frequently been reported, clearly indicating the occurrence of significant departures from equilibrium.

For these reasons, and because of their relative low cost and ease of operation, intrusive techniques continue to be widely used in the analysis of turbomachines. Among the many instruments for temperature, pressure, and velocity measurements [Fiock and Dahl, 1953], only thin films, aerodynamic probes and hot wires have frequency responses in the 10 kHz range, sufficiently high for resolving turbulent fluctuations in high speed turbomachinery flows. Hot wire anemometry, in all its variations, is a popular technique but is far too fragile to survive the hostile environment of gas turbine combustors. Using semiconductor transducers, in flush-mounted arrangements, aerodynamic probes are capable of measuring the pressure with bandwidths up to 50 kHz, quite adequate for resolving the most significant portion of the turbulent fluctuation spectrum [Biagioni and d'Agostino, 1999; Moss and Oldfield, 1990, 1991, 1992, 1996]. Similar frequency responses have also been obtained in temperature measurements using the aspirating probes originally developed by Ng and Epstein [Ng and Epstein, 1983]. Significantly better performance (up to 180 kHz) has recently been attained by Buttsworth and Jones [Buttsworth and Jones, 1996, 1997a] with a novel type of thin-film probe in air flows at moderately elevated temperatures and pressures (440 K, 4.6 bar). With respect to competing alternatives, this solution presents a number of important advantages, including robustness, ease of operation and independence from the properties and composition of the flow.

For the present study two intrusive probes where designed, calibrated and used. The first, for pressure fluctuations, was based on semiconductor transducers whilst the second, for unsteady heat transfer rates and temperature fluctuations used thin-film thermometer techniques. Each probe was mounted on a fast injecting device which allowed the probe to travel 100 mm inside the combustion chamber outflow in about 100 ms, which limited immersion times to sustainable levels.

The approach was based on the transient techniques developed by Oldfield, Jones and co-workers at Oxford University. The probes were developed and tested at Oxford University in collaboration with Consorzio Pisa Ricerche, Centrospazio laboratory, Pisa, Italy, and Syracuse University. Final high-pressure tests were conducted on a combustor at ENEL Produzione Combustor Research Centre in Sesta, Italy.

2.1 Pressure probe

Work at Oxford University in the United Kingdom has evolved a fast traversing Pitot probe and related instrumentation capable of measuring turbulence levels and spectra at frequencies in the range 100 Hz - 20 kHz, using an innovative transient technique [Moss and Oldfield, 1990, 1991, 1992, 1996]. In order to attain the required frequency response, the probe uses a Kulite fast sub-miniature semiconductor pressure transducer (Kulite model XCW 062/15) in a flush-mounted arrangement, which minimizes the inlet line impedance and resonance. The sensing diaphragm is protected from the hot flow by means of an inlet screen to prevent particle impacts and by a layer of silicone rubber to shield it from direct contact with high temperature gases. By traversing the probe rapidly through the hot flow and hence reducing the duration of the probe exposure to the hot steam, Moss and Oldfield [Moss and Oldfield, 1991] demonstrated the possibility of measuring the turbulent pressure spectrum at the exit of a combustor operating at atmospheric exit pressure and temperatures up to 1500 K. (Figure 1) In these conditions the residence time of the probe in the hot flow had to be limited below about 80 ms, in order to prevent biasing errors and irreversible damage due to the transient temperature rise of the sensing element (Figure 2). The measurement yielded useful spectral information in the frequency range from 20 Hz up to 20 kHz, more than adequate for effective characterization of the turbulence structure at the gas turbine inlet.

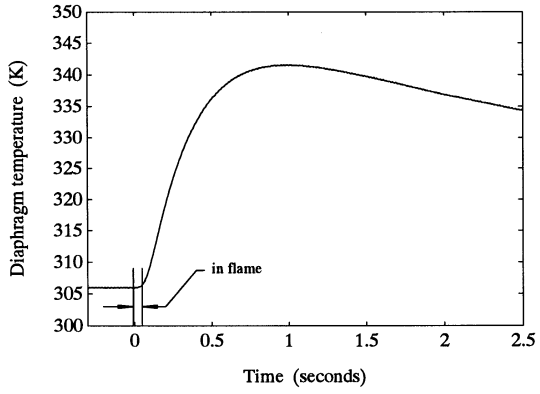

Figure 1 Previous experience with pressure probes in a hot flow: temperature rise of the transducer, during and after exposure to the flow [Moss and Oldfield, 1991].

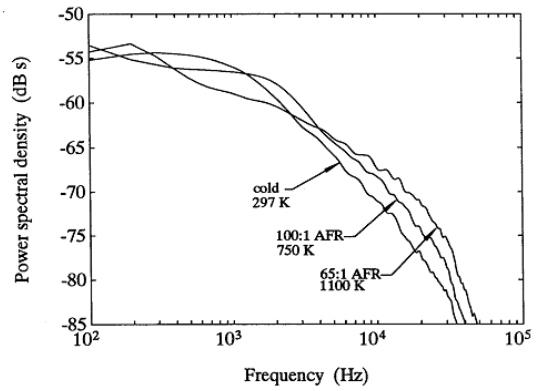

Figure 2 Previous experience with pressure probes in a hot flow: typical turbulence frequency spectra [Moss and Oldfield, 1991].

In the present application, to ensure geometric compatibility with the ENEL combustor and the injection mechanism, a new probe head had to be designed. It was mounted in an 8 mm OD stainless steel tube designed to be slipped inside the 10 mm OD main piston rod of the injection mechanism and secured with machine screws. (Figure 3)

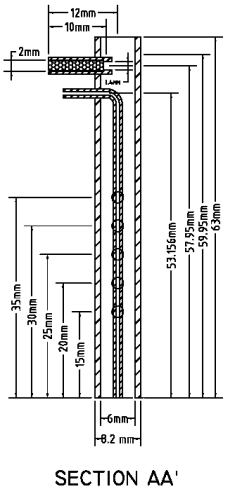

Figure 3 Pressure probe scheme.

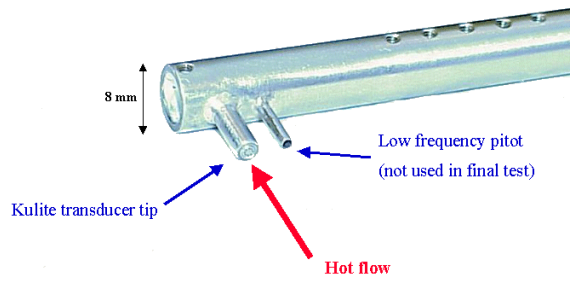

Figure 4 Pressure probe detail.

Two versions of the probe were manufactured: one based on a Kulite XCQ–062–5D differential transducer which used a low frequency Pitot to retrieve dynamic head, and one based on a Kulite XCQ–062-150PSIA absolute transducer (1.6 mm diameter, with Paralene coated diaphragm and B-screen) which was used in the final test because it was better able to stand starting pressure fluctuations. The installed transducer (serial n. 5307–2A–143) has a sensitivity of 0.778 mV/psia with an excitation voltage of 5 V, which is equivalent to 27 mV/bar at 12 V excitation in the present arrangement. (Figure 4) The probe measures the total pressure $P_0(t)$ which, can be expressed as the sum of the instantaneous static pressure and the instantaneous dynamic pressure:

$$P_0 = p + \frac{1}{2}\rho u^2 = \bar{p} + p' + \frac{1}{2}(\bar{\rho} + \rho')(\bar{u} + u')^2$$

where $\bar{p}$, $\bar{u}$ are time-mean static pressure and velocity components and p', u' are the equivalent unsteady perturbations.

It can be shown [Moss and Oldfield, 1990] that, given a number of assumptions that seem well-justified in low Mach number, modest turbulence intensity flows, this formula can be reduced to one defining the velocity fluctuations as a linear function of the total pressure fluctuations:

$$\frac{u'}{\bar{u}} = \frac{1}{2}\frac{P_0'}{(\bar{P}_0 - \bar{p})}.$$

The main assumption is that density fluctuations are small compared to the velocity fluctuations and is justified because, for small-scale disturbances, conductivity will rapidly damp out temperature differences.

Once velocity fluctuations are retrieved, turbulence spectral analysis can be performed via standard methods obtaining turbulence intensity and length scale. In practice, the sensitivity of the pressure probe to turbulent flow fluctuations is calibrated against a hot-wire in a room temperature wind tunnel with grid/bar turbulence, and the above equation is replaced by a frequency and wavenumber dependent version [Anthony *et al.*, 1999; Biagioni and d'Agostino, 1999; Moss and Oldfield, 1990].

The prototype probe was tested at NASA's Glenn Research Center during 2001. Hot wire data was collected behind two different turbulence-generating square-bar grids (one half-inch bars, the other quarter-inch), and then compared with Kulite data taken in the same positions behind the same grids. Downstream distance from the grids was between 20 and 40 bar diameters. Turbulence spectrum appears to be close to the hot wire one in the midfrequency range, while a bigger difference can be seen both at low and high frequencies. (Figure 5) Furthermore, as for Moss and Oldfield's works, it appears that turbulence length scale, calculated using the inverse Fourier transform of the power spectrum, is overestimated for Kulite data: calibration for each single probe is therefore needed in order to compensate errors due to resonance frequency of transducer diaphragm and probe size.

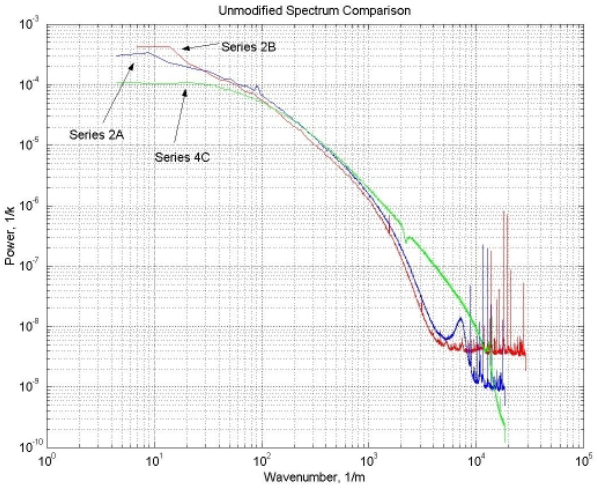

Figure 5 Comparison of relevant wavenumber spectra for calibration of series 2 ½ inch data before any modifications. Series 2A and 2B are Kulite probes, 4C is a hot wire.

As for Moss and Oldfield, two calibration functions can be found, one in wavenumber space, the other in frequency space: the Kulite measured spectrum $M(k,f)$ is supposed to be related to the real spectrum $S(k,f)$ by the two calibration functions $G_1(k)$ and $G_2(f)$ as expressed in the following equation:

$$M(k,f) = S(k,f)\cdot G_1(k)\cdot G_2(f)$$

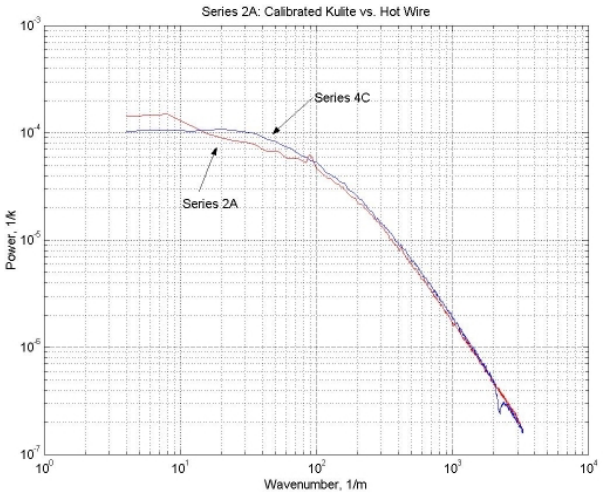

Figure 6 Calibrated version of series 2A (½ inch grid, 34 m/s) versus hot wire data for the same flow. Truncated to probe resolution.

Comparing Kulite spectra to the hot wire ones, considered correct, it is possible to determine the unique calibration curve for the specific probe. (Figure 6) In the present case it appeared that only the wavenumber calibration function was needed, because frequency effects are small: the procedure was applied to the prototype results leading to a correct estimate of turbulence parameters, with difference between hot-wire and Kulite readings of the order of the probe size, and therefore of probe resolution (Table 1).

Designation	Length Scale Before Cal. (m)	Length Scale After Cal. (m)	Length Scale Ratio	Absolute Error
Series 2A	0.019	0.011	1.7	0.0018
Series 2B	0.026	0.010	2.6	0.0005
Series 2C	0.012	0.007	1.6	0.0006
Series 2D	0.037	0.005	7.2	0.0017
Series 3A	0.020	0.011	1.8	0.0020
Series 3B	0.027	0.010	2.7	0.0002
Series 3C	0.013	0.008	1.6	0.0015
Series 3D	0.037	0.005	7.3	0.0019
Series 4A	0.0065	0.0065	NA	NA
Series 4B	0.0069	0.0069	NA	NA
Series 4C	0.0092	0.0092	NA	NA
Series 4D	0.0096	0.0096	NA	NA

Table 1 Calibration procedure results for all Kulite data. Absolute error is ABS(HW-Kulite). Length scale ratio is the ratio of length scale before calibration to that after calibration

2.2 Temperature probe

In 1997 Buttsworth and Jones [Buttsworth and Jones, 1996, 1997a; Buttsworth *et al.*, 1998] developed a new miniature twin hemisphere heat transfer probe capable of measuring unsteady total temperature fluctuations up to 180 kHz, as well as the mean total temperature profile. The probe consists of two quartz hemisphere-cylinder assemblies, equipped with platinum thin film gauges at the two stagnation points and electrically heated at different wall temperatures T_{w1} and T_{w2}. Except for negligible viscous dissipation effects, the recovery temperature at the stagnation points practically coincides with the total temperature T_{tot} of the flow.

$$q_1 = h\left(T_0 - T_{w1}\right) \qquad \text{and} \qquad q_2 = h\left(T_0 - T_{w2}\right)$$

where the heat transfer coefficient h is a very weak function of the wall temperature and can be assumed constant for both gauges. Elimination of h between these equations allows one to determine the total temperature:

$$\left.\begin{aligned} \dot{q}_1 &= h\cdot(T_{tot} - T_{w1}) \\ \dot{q}_2 &= h\cdot(T_{tot} - T_{w2}) \end{aligned}\right\} \Rightarrow \quad T_{tot} = \frac{T_{w1}\dot{q}_2 - T_{w2}\dot{q}_1}{\dot{q}_2 - \dot{q}_1}$$

Instantaneous total temperature recovery was therefore possible (Figure 7) once the films started with two different initial temperatures (T_{w1} and T_{w2}): this was accomplished using a pre-heating circuit for one of the films.

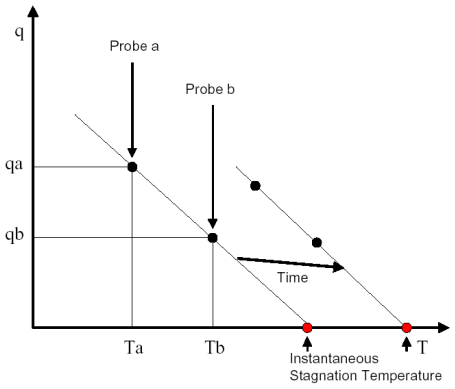

Figure 7 Recovery of stagnation temperature from two temperature heat transfer measurements.

In the present application, though, fast injection of the probe and the necessity to operate in a hostile environment led to a different approach in temperature probe design which both avoided the complexity of the heating circuit and at the same time made the probe more rugged: *the self-heating two-substrate temperature probe*.

The two films were deposited on geometrically identical cylinders made of different ceramic materials in order to naturally create a difference in temperature due to the hot flow. (Figure 8) Film temperature rises as a function of the substrate material $\sqrt{\rho c k}$: cordierite and quartz were therefore chosen because they have similar thermal diffusivity and hence similar thermal penetration depths, but sufficiently different temperature rises. Considering nominal conditions (p = 20 bar and T_{tot} = 1500 K) and 100 ms immersion time, the theoretical calculated temperature difference was of about 300 K. (Figure 9)

Material	density, ρ (kg/m^3)	c (J/kgK)	k (W/mK)	sqrt(ρ*c*k)	diffusivity (m^2/s)
Quartz	2210	755	1.4	1528.39	$8.39 \cdot 10^{-7}$
Cordierite	2600	1464.4	3.0	3379.69	$7.88 \cdot 10^{-7}$

Table 2 Substrate material properties

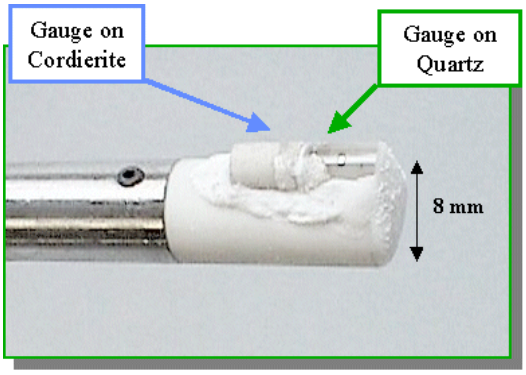

Figure 8 Detail of temperature probe head.

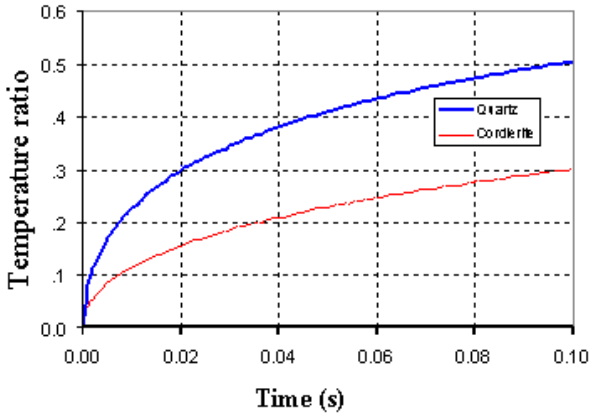

Figure 9 Theoretical temperature rises for the two films: temperature ratio is defined as $(T - T_i)/(T_{tot} - T_i)$

Once total temperature history is retrieved, temperature fluctuations can be retrieved via the standard methods [Buttsworth and Jones, 1996].
The probe was designed (Figure 10) to fit on the same piston rod as the pressure probe with the substrate cylinders (4 mm diameter) mounted on a hollow MACOR® cylinder with an internal thermocouple. After extensive research, ceramic parts were mounted with a high temperature ceramic adhesive capable of withstanding the mechanical and thermal stresses associated with the unsteady injection.

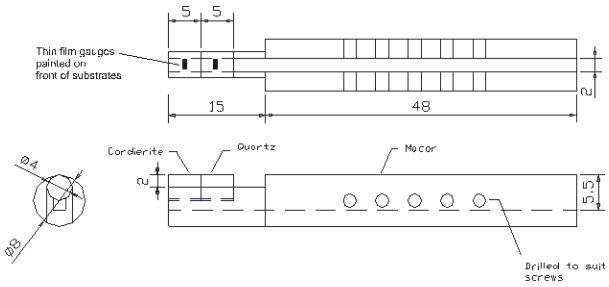

Figure 10 Temperature probe scheme.

Four probes were manufactured and, initially, calibrated at Oxford using the Oxford Step Heating calibration facility using heat gun and gas torch flows. This experiment was intended to resolve some uncertainty regarding the actual thermal properties of the cordierite sample.

Probe	Quartz film Res. @ 20°C	Quartz film slope	Quartz film alpha	Cord. Film Res. @ 20°C	Cord. Film slope	Cord. Film alpha
Prot.	20.815	0.0356	$1.71 \cdot 10^{-3}$	25.980	0.0604	$2.31 \cdot 10^{-3}$
#1	20.641	0.0420	$2.04 \cdot 10^{-3}$	41.505	0.0981	$2.36 \cdot 10^{-3}$
#2	27.465	0.0402	$1.46 \cdot 10^{-3}$	37.087	0.0977	$2.63 \cdot 10^{-3}$
#3	20.659	0.0452	$2.18 \cdot 10^{-3}$	22.691	0.0605	$2.66 \cdot 10^{-3}$

Table 3 Film calibration results for the four manufactured probes

3. Injection mechanism

In order to reduce probe residence time inside the combustor hot flow, a probe injection mechanism was designed [Torre, 1999; Pondicq-Cassou, 2001] with the following specifications:

- nominal maximum penetration: 100 mm
- nominal traverse time: 100 ms
- ambient pressure: up to 30 bar
- injection remotely controlled via software
- traverse time adjustable via software

Different techniques were evaluated, resulting in the choice of a pneumatic device with injection driven by the motion of a piston in a pressurized cylinder, (Figure 11) the compressed air flow being controlled by 4 SMC fast solenoid valves.

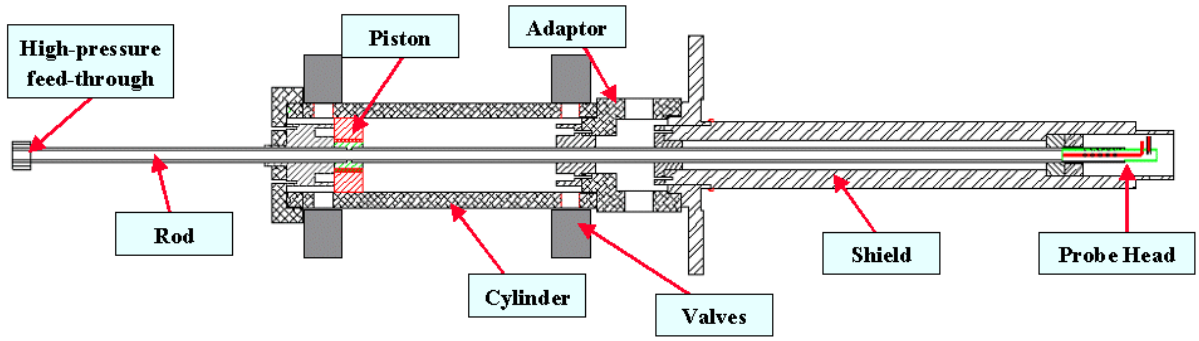

Figure 11 Injection mechanism scheme.

	Material [-]	Length [mm]	Inner Diameter [mm]	Outer Diameter [mm]	Notes
Rod	Al 6061-T6	740	8.25	9.5	
Cylinder	AISI 304	208	50	70	
Piston	Al 6061-T6	19.45	9.5	48.4	Weight: 40 g
Shield	AISI 1018	340	19	45	Ends with flange B16.5
Adaptor	AISI 1018	67	---	75	
Piston Stops	Phospor Bronze	19	---	41	Holding steel springs and PTFE disks
Probe holder	Al 6061-T6	63	6	8.2	

Injection mechanism total length	780 mm
Injection mechanism total weight	~ 10 kg

Table 4 Injection mechanism components

The necessity of surviving the hostile combustor environment permeated every detail of the design. To facilitate combustion chamber attachment, a steel shield (including an ANSI flange welded to one end) and cooling system adaptor were added along with an external shield provided by ENEL and directly connected to the rig. The shield is a simple 13.5 inch tube designed to protect internal components from heat generated at the walls of the combustor and to direct coolant out to the Kulite. Coolant is fed through compression fittings on the adaptor, which is threaded onto the back of the flange/shield assembly [Pondicq-Cassou, 2001]. This adaptor provides part of the cooling capacity, with a supplement supplied directly on the rig, outside of the shield and also with the possibility to provide a little cooling directly to the probe head via the piston rod. For simplicity, all of the cooling flows are controlled by choked orifices in order to provide a constant mass flow rate independent of combustor pressure.

To ensure that the mechanism could handle the pressures associated with the combustion chamber, an extensive series of pressure tests were carried out at Syracuse [Torre, 1999] using a steel pressure cap threaded onto the end of the shield. This allowed the entire shield and piston rod to be pressurized using the

cooling system ports. Using this method, the primary pressure seal, located just behind the shield where it emerges from the combustion chamber, was tested up to 35 bar, and the injection system itself was operated with the shield pressure as high as 32 bar without incident. Over 200 pressure test cycles were run, in addition to injection tests at both atmospheric and elevated pressure. These tests included some with a complete Kulite probe head assembly which emerged unharmed. The following tables illustrate the best performance for cases with and without background pressure: in these tables, phase 1 is the insertion, phase 2 is the retraction; *Max* is the maximum penetration distance in one direction; total traverse is the time to complete the round trip out to the max value and back; flow time is the time the probe would have spent exposed to the combustion air, which accounts for the 20 mm the probe was inside the shield on the insertion and retraction.

As shown, operating at elevated pressure slows the injection time due to the increased pressure force applied to the end cap attached to the piston rod (where the wiring and pressure feed-throughs are located). Variation in background pressure changed maximum penetration by only about 1%, and injection time by less than 10%

The impact shock of the piston on the forward stop created a noise spike on the position signal due to a slight resonance in the transducer mounting and coupling with interference due to valve activation (Figure 12).

Cyln. Pressure (bar)	Shield Press. (bar)	Pulse Width (s)	Total Traverse (s)	Max (mm)	Flow Time (s)	Phase 1 Time (s)	Phase 2 Time (s)	Phase 1 speed (m/s)	Phase 2 Speed (m/s)	Averag e Speed (m/s)
8.3	0	0.08	0.128	129	0.105	0.067	0.062	1.82	-2.24	2.03
9.0	0	0.08	0.128	130	0.105	0.067	0.062	1.83	-2.22	2.02
9.7	0	0.085	0.136	129	0.113	0.072	0.064	1.70	-2.19	1.94
10.3	0	0.085	0.137	130	0.113	0.072	0.065	1.70	-2.16	1.93

Cyln. Pressure (bar)	Shield Press. (bar)	Pulse Width (s)	Total Traverse (s)	Max (mm)	Flow Time (s)	Phase 1 Time (s)	Phase 2 Time (s)	Phase 1 speed (m/s)	Phase 2 Speed (m/s)	Average Speed (m/s)
130	200	0.095	0.147	128	0.116	0.081	0.066	1.55	-2.13	1.84
140	300	0.1	0.150	128	0.117	0.085	0.065	1.49	-2.12	1.81
130	370	0.11	0.155	130	0.125	0.090	0.065	1.39	-2.18	1.79
130	450	0.095	0.135	130	0.107	0.077	0.058	1.64	-2.37	2.00

Table 5 Best injection runs for different cylinder operating pressures (up) and for different back-pressures (down)

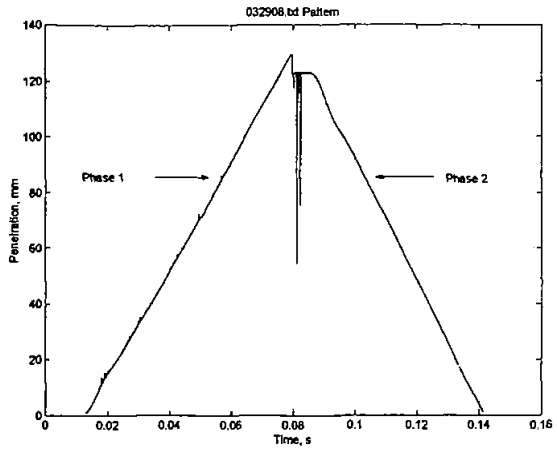

Figure 12 Position sensor signal during a traverse.

Overall, however, the performance of the injection mechanism is very stable, reliable and repeatable. Relatively large changes in reciprocating mass have very little effect on the injection times which greatly increases versatility when using more than one probe.

After the first hot test session in Sesta facility (June 2001), some design changes were made to the injection mechanism, mainly to increase its durability at high temperature:

- Replacement of all low temperature plastic parts with metal ones (new piston design) and minimal PTFE seals.
- Use of stainless steel where possible

These changes slightly modified the injection performance. (Figure 13) The improved injection mechanism was successfully bench-tested at Centrospazio:

- Maximum penetration distance was 96% of the prototype
- No difference on injection times
- Reduced effect of piston impact

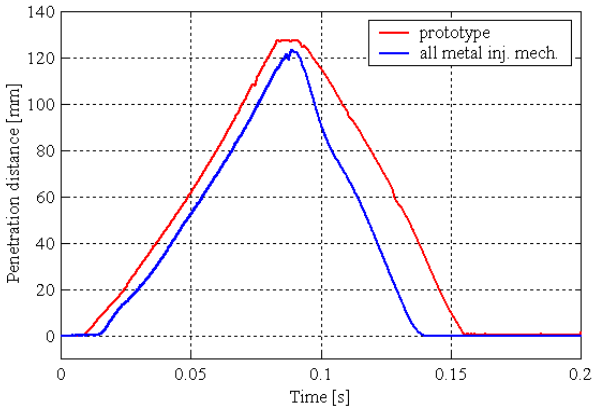

Figure 13 New injection mechanism: injection performance compared with the prototype.

4. Cooling system

The original cooling system [Battelle, 2001; Pondicq-Cassou, 2001] included three different, orifice controlled cooling flows: the first flowing between the external ENEL shield and the probe shield, the second inside the probe shield, and the third, much smaller, inside the piston rod. After the first hot test session in June 2001, which showed some issues with heat transferred from the rig wall to the probe, orifice cooling mass flow was increased and two "dummy" tests (Jan-Mar 2002) were performed in order to assess cooling effectiveness. (Figure 14) The possibility of increasing the insulation by wrapping insulating ceramic paper around the probe shield was also evaluated during the two dummy tests.

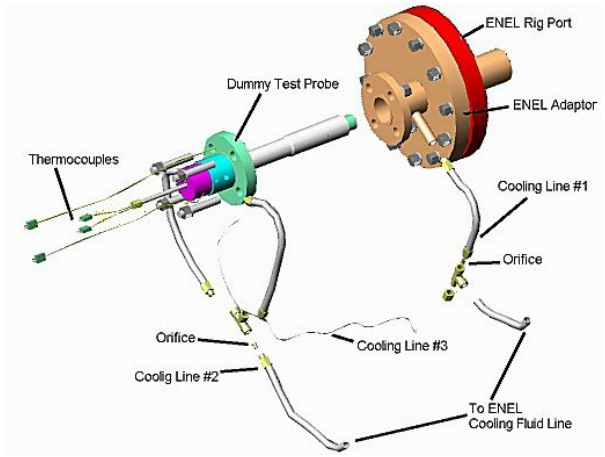

Figure 14 Dummy test set-up scheme.

The probe was tested in Sesta with full cooling, no injection and thermocouples mounted in place of probe head and at several points along the probe body. (Figure 15)

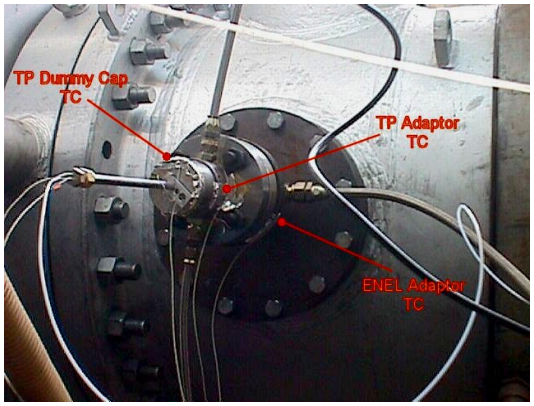

Figure 15 Dummy test probe mounted onto the rig with highlighted external thermocouple placement.

Dummy Test 1 was carried out on 8 January 2002, with 5 thermocouples mounted on probe and injector and insulating paper. The Sesta rig was run continuously for 4 hours with pressures up to 15 bar and temperature up to 1500 K: (Figure 16)

- temperature at probe position never exceeded 22 °C
- temperatures on injection mechanism never exceeded 18 °C.

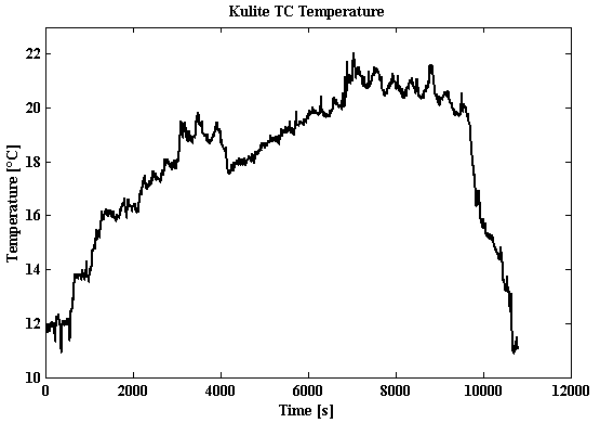

Figure 16 Temperature history for the "probe-head" thermocouple during Dummy Test 1.

Dummy Test 2 was carried out on 21 March 2002, with 4 thermocouples mounted in probe and injector and without insulating paper. The Sesta rig was run continuously for 3 hours with pressures up to 16 bar and temperature up to 1400K:

- temperature at probe position never exceeded 30 °C

The dummy tests showed that the cooling system was now more than adequate to keep the probe cooled in the retracted rest position.

5. Data acquisition and post-processing

Due to safety constraints, no one is admitted in the test cell in Sesta when the rig is running. Consequently, probe injection has to be remotely controlled: this is achieved through software written in National Instruments's Labview 5.01 environment [Battelle, 2001]. Injection software also controls the valve opening; the valves are powered via a miniaturised solid state relay commanded directly by the DAQ board. Finally, the same board and software acquire and write pressure/temperature signals. The whole system is based on National Instruments PCI-6071E data acquisition boards installed on a standard PC computer; 5 data channels are acquired for the pressure probe, 6 for the temperature probe with bandwidth up to 200 kHz for each channel. Additional constraints on data acquisition were posed by the highly electrically noisy environment in Sesta and the long (~ 16 m) BNC cables that had to be used between test cell and control room: particular care was therefore devoted to pre-amplifier design.

Both the pressure and thin-film gauge differential preamplifiers use the Analog Devices SSM2017 chip (now replaced by the SSM2019) which was designed for use as a microphone pre-amplifier. These chips are optimized for low noise with low source impedance and have a wide bandwidth and low distortion. They are well suited from a noise point of view to the low impedances of pressure transducers (typically 500 – 900 Ω) and thin film gauges (typically 20 – 50 Ω). Both pre-amplifiers include a differential input DC amplifier, an AC coupled amplifier, and a low-pass anti-aliasing filter. Problems were encountered with driving the ~16 m cables to the control room, and R10 and R11/C11 were added to both circuits to prevent oscillations due to the large effective load capacitance.

Similar but slightly different circuits are used for pressure (Figure 17) and temperature (Figure 18) probes. The pressure transducer amplifier has a flat frequency response but the thin-film gauge amplifier boosts the higher frequencies (Figure 19) of the thin film gauges, to reduce digitisation errors as the thin - film voltage signal falls with increasing frequency.

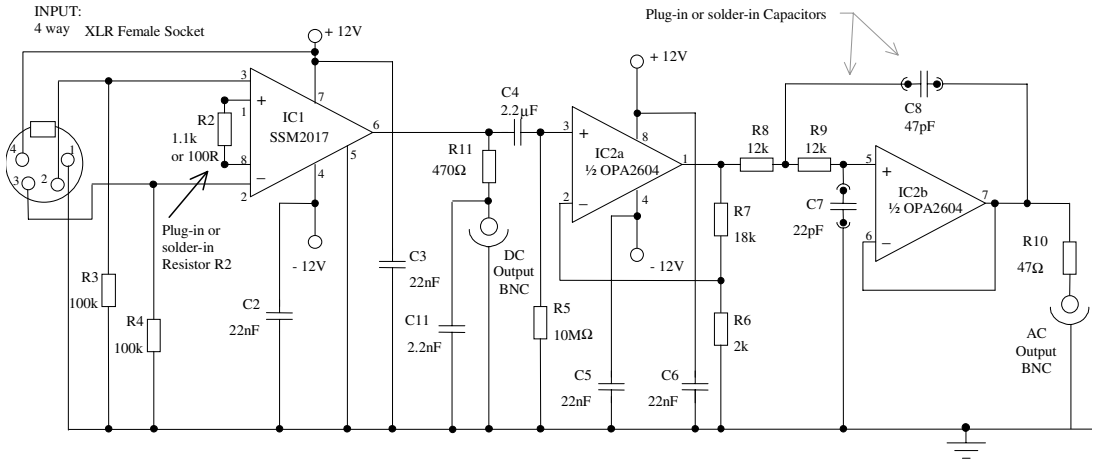

Figure 17 Single Channel of Pressure Transducer Signal Conditioning Unit.

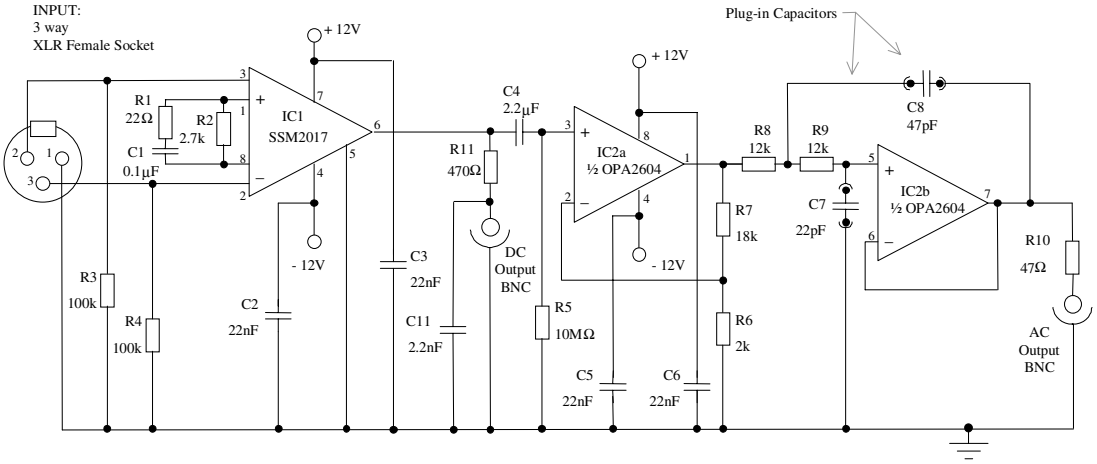

Figure 18 Single Channel of Thin Film Gauge Array Signal Conditioning Unit

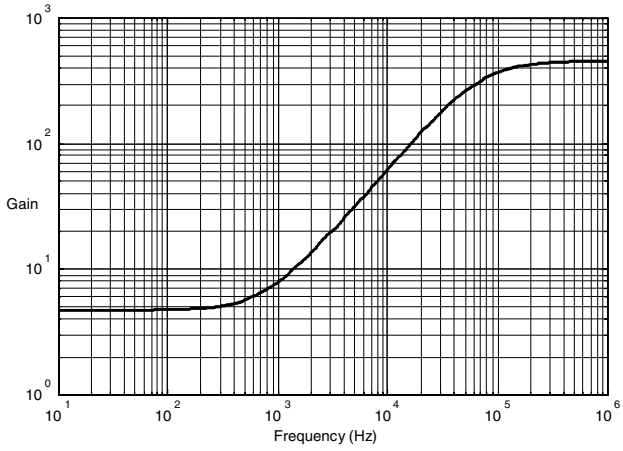

Figure 19 Theoretical frequency response of thin-film gauge amplifier showing high frequency boost used to reduce digitisation errors.

The thin-film gauge amplifier high frequency boost must be subsequently removed by digital processing to recover the thin film gauge temperature signal and hence the heat transfer signal [Oldfield, 2000]. Different outputs can be simultaneously retrieved from both amplifiers to accommodate a wide dynamic range in the input signals and to maximize signal-to-noise ratio at various frequencies: DC ×10, AC ×100, and AC ×1000 gain for pressure signals; DC ×4.7 and variable AC gain for thin-film gauges. The final amplifier unit, designed and manufactured at Oxford University, consists of 8 separate channels, each providing a DC and an AC output (6 are used for pressure probe, 2 for temperature probe). In addition to the preamplifier box, a DC current supply and a constant current source for thin film gauges (Figure 20) were designed and manufactured at Oxford.

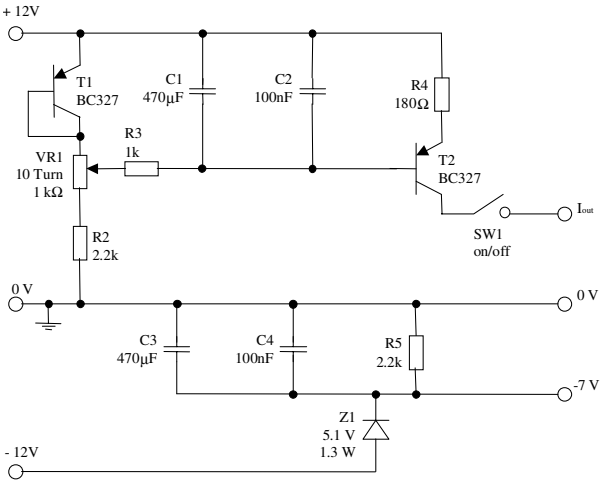

Figure 20 0–20 mA constant current source used with thin film gauges.

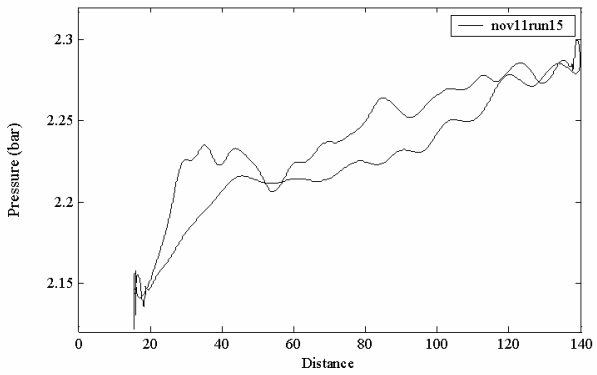

Figure 21 Low-pass filtered pressure trace.

Looking at the low-pass filtered pressure trace (Figure 21) there is a sharp rise in pressure as the probe leaves the cooling shroud followed by a gradual rise as it moves towards the combustor exit flow. It is difficult to tell whether any point here is effectively at zero velocity i.e. whether the influence of the coolant flow finishes before the total pressure starts to rise at the edge of the jet.

Looking at the low-frequency perturbations as the jet moves from side to side across the probe tip we see a typical amplitude of approximately one quarter of the nozzle exit dynamic pressure. (Figure 20)

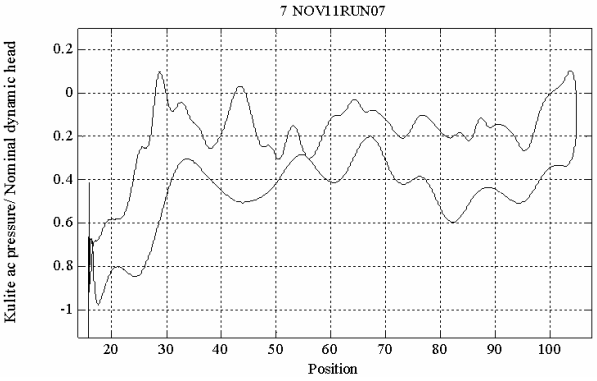

Figure 22 Kulite low-frequency perturbation amplitude compared to nozzle exit dynamic pressure.

There was some run to run variation in this amplitude but this would appear to be due to variations in the jet trajectory rather than a change in the jet divergence angle. The time-mean dynamic pressure at the probe location, $\overline{P}_0 - \overline{p}$, was accordingly taken for all runs to be ¼ the nominal value in the discharge nozzle; the equivalent jet velocity is ½ of the nozzle velocity.

5.1 Pressure probe

Pressure fluctuations are derived from the Kulite voltage measurements using the quoted transducer sensitivity; the pressure fluctuation signals are then converted to a velocity fluctuation using $\frac{u'}{\overline{u}} = \frac{1}{2}\frac{P_0'}{\left(\overline{P}_0 - \overline{p}\right)}$. This conversion is clearly sensitive to the mean dynamic pressure, $\overline{P}_0 - \overline{p}$, which is difficult to define precisely in the Sesta flowfield with the transducer on the edge of a jet flow which was found to exhibit a low frequency "flapping" motion. Two methods were investigated to estimate this mean dynamic pressure level for each run:

- The rise in peak pressure as the transducer entered the jet
- The peak to peak amplitude resulting from the jet motion, with the transducer periodically exposed to jet flow and no-flow conditions.

The facility provides mass flow, temperature and pressure data, for each run together with the cross-sectional area of the combustor discharge nozzle. This allows one to calculate a "nominal" dynamic pressure at this point. The jet will, however, diverge as it moves through the instrumentation chamber (Figure 34) and the effective dynamic pressure must thus be smaller than at the nozzle exit plane.

Pressure data was sampled at 100 kHz and the signal from the ×100 amplifier was used to minimise digitisation noise and cross-talk. The Welch power spectrum algorithm was used to obtain spectra from the signal for the time in which the probe was inserted beyond the noise from the cooling flow. Comparing this spectrum with one from a no-flow noise test shows that there is an excellent signal to noise ratio. (Figure 23)

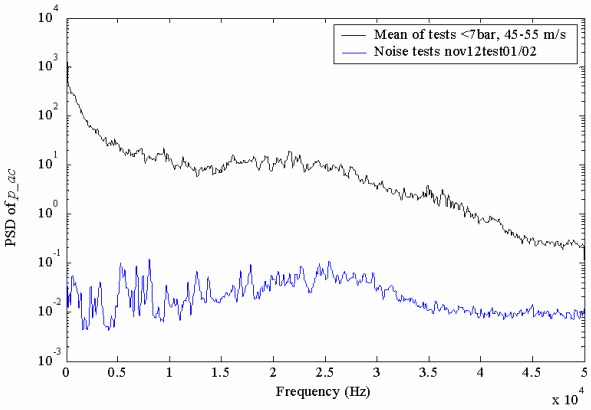

Figure 23 Measured electrical noise compared with measured signal in Sesta.

Spectra at the same condition are ensemble-averaged to reduce the random noise component (inherent in any sample of a random signal) and can be plotted either against frequency or wavenumber domains, where the wavenumber is defined as $k = \frac{2\pi f}{\bar{V}_{jet}}$. At similar conditions (nominal exit velocity 110 m/s, (Figure 24) there is little non-random run to run variation in the spectra and they may safely be ensemble-averaged.

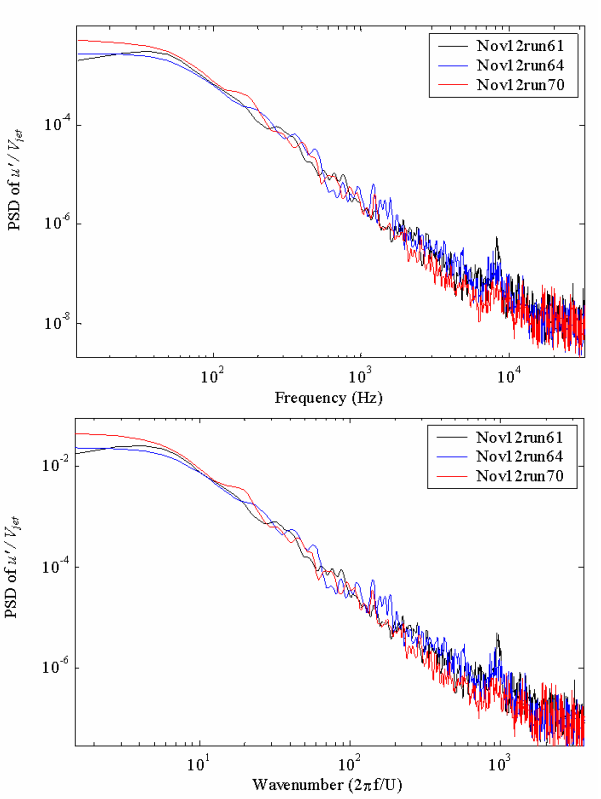

Figure 24 Power spectral density of the pressure probe signal, plotted against frequency and wavenumber.

Estimates of the turbulence integral length scale are obtained from autocorrelations of the unsteady velocity signal, with autocorrelations from similar tests being ensemble-averaged. The length scale is obtained by integrating the area under the curve in one of the positive quadrants: $\Lambda_x = \bar{V}_{jet} \int_0^{R=0} R(\tau) \mathrm{d}\tau$

In practice the autocorrelations of the Sesta data exhibited two features that seriously affected the accuracy of this calculation: (Figure 25)

- Some of the autocorrelations had a sharp central spike indicative of random noise. This does not appear to be electrical interference; instead it is thought to be acoustic in origin. The automatic scaling of the autocorrelation, to give a peak amplitude of 1, reduces the area under the curve if such a spike is present. Future probes will have a fixed, microphone transducer to determine whether this is in fact the case; the acoustic component could then be subtracted from the spectrum and the autocorrelation obtained from the spectrum rather than the time-domain signal.

- Some autocorrelations resembled a cosine wave and were clearly dominated by the low-frequency "flapping" motion of the jet. The resulting length scale refers more to the flapping motion than to the structure of the turbulence.

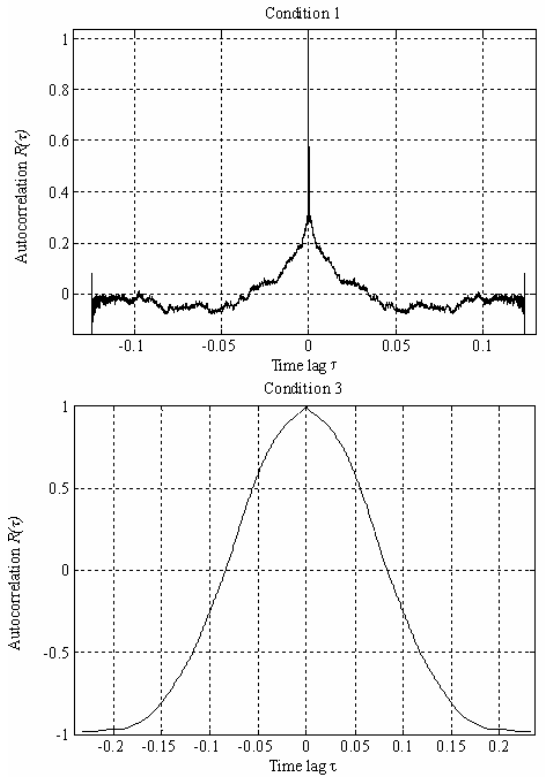

Figure 25 Autocorrelation features: sharp central spike (up), cosine wave shape (down).

5.2 Temperature probe

The temperature probe is connected to two channels of the fore-mentioned amplifier box, one for the quartz film and one for the cordierite film. Dedicated DAQ and post-processing routines were written in the Labview and Matlab environments. (Figure 27) Extensive calibration was performed, both in Oxford and at Centrospazio in order to identify the new probe design characteristics and proper post-processing. The final post-processing routine was able to identify and overcome all the remaining uncertainties, related to individual probe and component characteristics and mutual interference.

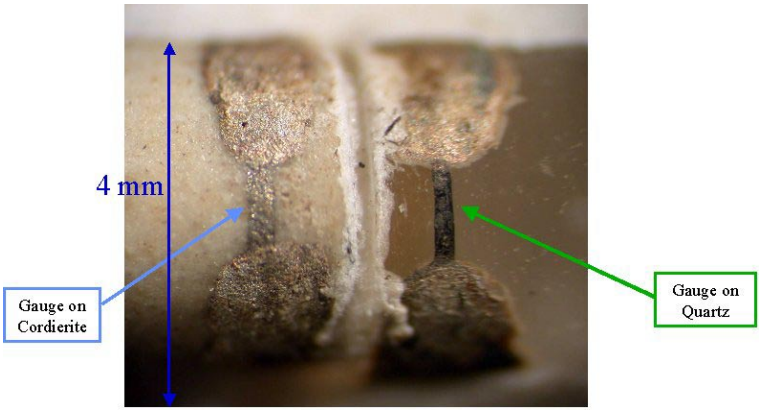

Figure 26 Close up of temperature probe after hot test.

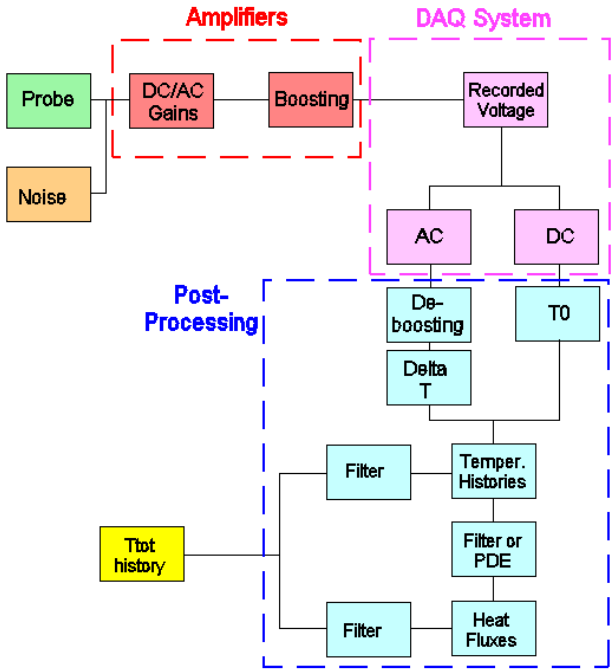

Figure 27 Temperature probe data processing algorithm.

In particular, after retrieving via standard methods the two film temperature histories, wall heat fluxes were determined in two different ways. The first [Buttsworth and Jones, 1997b] uses quasi-infinite flat plate approximation and then corrects the obtained value for two-dimensional effects due to cylindrical shape of the probe (lateral conduction) with the following formula:

$$q = q_{1d} - \frac{k \cdot (T_{film} - T_{initial})}{D}$$

The second method retrieves heat flux directly from the temperature distribution inside the ceramic cylinder, using a numerical solution of the PDE heat transfer equation in the form of an implicit finite difference code, 2nd order accurate in space and time, developed at Centrospazio (Figure 28)

Results were practically identical for the two techniques, showing that two-dimensional effects were indeed significant, altering wall heat flux up to 15%. (Figure 29)

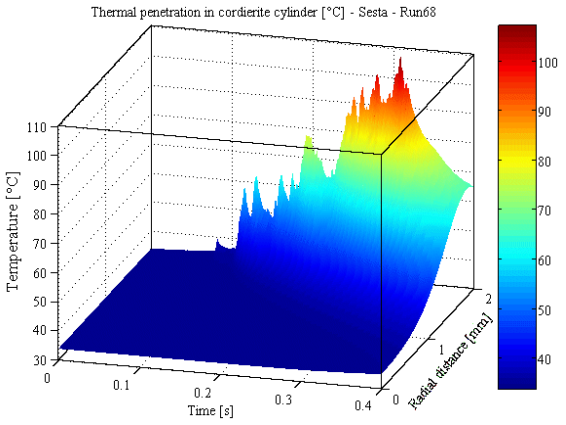

Figure 28 Temperature field inside the cordierite cylinder during a run.

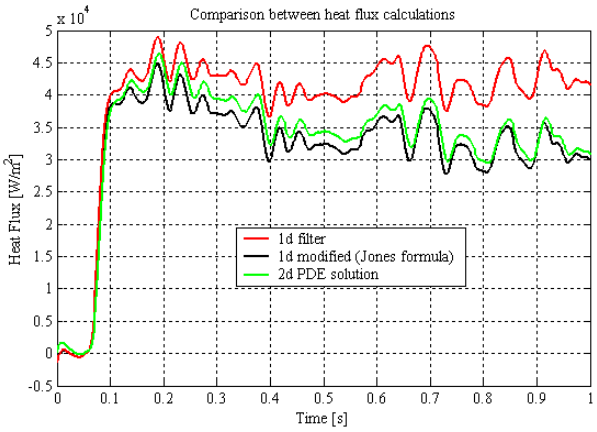

Figure 29 Comparison of radial conduction effects on heat flux computed with the two methods.

Calibration was completed using firstly, heat gun and gas torch (Figure 30, Figure 31, Figure 32) flows directly on the probe and then repeating the process after mounting the probe on the injection mechanism, in order to verify also its resistance to injection mechanical shocks. The results showed that probe, and in particular its critical components (films and ceramic adhesive) were able to survive injection in high-temperature flows, (Figure 26) providing, after a settling time in the order of 5–10 ms (due to the fact that films start at the same temperature), accurate instantaneous total temperature history, with bandwidth up to about 30 kHz.

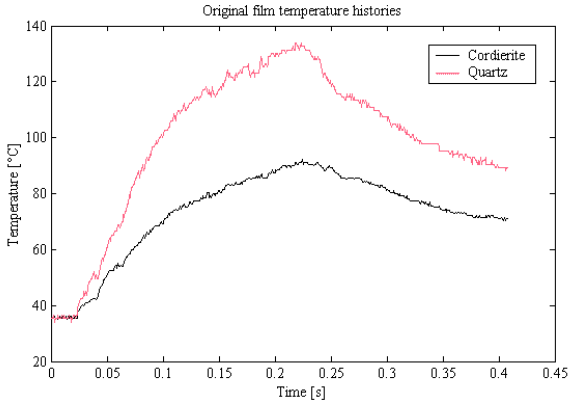

Figure 30 Typical temperature history for the two films.

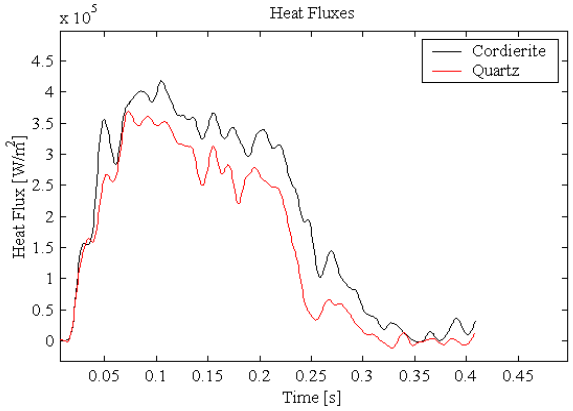

Figure 31 Typical heat flux history for the two films.

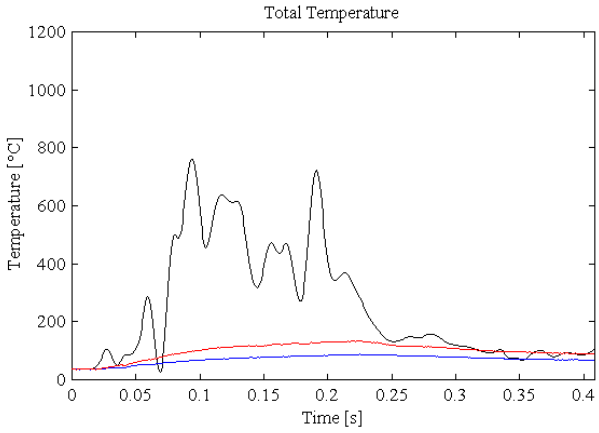

Figure 32 Typical retrieved total temperature history for a gas torch run.

6. Testing facility

ENEL (Ente Nazionale Energia Elettrica) is the largest Italian power generating company and the second largest in Europe. ENEL Produzione's Sesta facility is located near Siena, in Italy. Operative since 1997, Sesta Gas Turbine Test Facility allows for testing of full scale combustion chambers and "hot" gas turbine components. Two identical test rigs can operate (alternately) with pressure up to 25 bar and mass flow rate up to 38 kg/s. The Syngas plant, in activity since 1998, allows for utilisation of non-conventional fuels and mixing of pure gases. The facility is presently used by many worldwide combustion chamber manufacturers and for ENEL's internal tests. ENEL can provide its customers with a wide measurement capability (flow parameters, exhaust gas composition, flame analysis) and interfaces for customer's own measurement devices (intrusive, optical etc.).

ENEL supported the present activity by providing an access point on the rig for the injection mechanism, directly downstream of the nozzle connected with the combustion chamber; ENEL provided also an adaptor to mate the injector to the rig and the high-pressure air line needed for cooling and injection operation; finally ENEL provided part of their test data in order to compare measurements and better characterize flow conditions around the probes.

The probe testing had therefore the advantage of accessing full-scale hot, high-pressure industrial combustors and piggy-backing industrial tests (at no cost) - although at the expense of limited flexibility in probe position and some scheduling limitations.

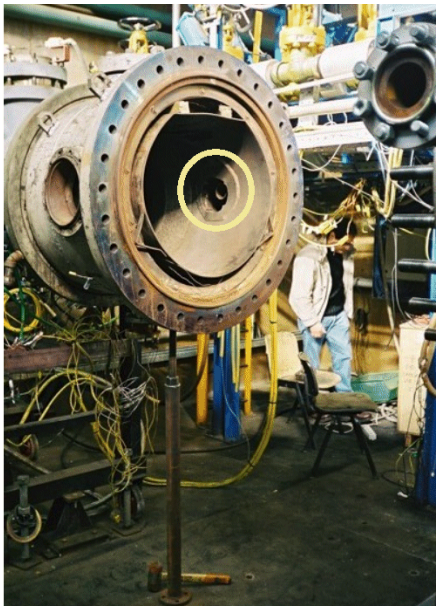

Figure 33 Probe insertion point (yellow circle) in Sesta cell 2 test rig.

7. Results

Final tests were carried out for both probes at the end of 2002: a two-day test window was used for the pressure probe on November 11th and 12th, while the temperature probe was tested on December 12th. Final probe positioning was not ideal due to the fact that the only usable access port (Figure 33) was approximately 0.5 m downstream of the combustion chamber exit nozzle (Figure 34) and allowed only limited penetration of the jet by the probe traverse: this notwithstanding, probes were used in the hot flow for several hours, performing successfully over 200 injections (150 for pressure probe, 90 for temperature probe): at the end of the test campaign, the pressure probe was still functioning, while the temperature probe had suffered major damage. A final problem was present in both test sessions: Sesta's air supply for the injection mechanism lacked sufficient pressure to obtain full probe penetration for the high-pressure runs.

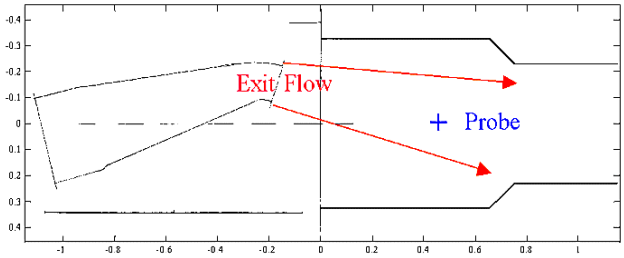

Figure 34 Schematic of probe positioning in Sesta (distance in m).

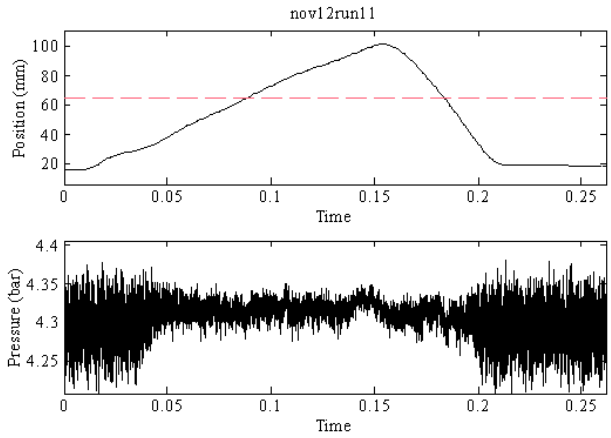

Figure 35 Typical injection pattern and recorded pressure signal for a Sesta run: change in rms level as the probe leaves the cooling shroud.

7.1 Pressure probe

The pressure probe hot test session was carried out in the Sesta facility on 11–12 November 2002. The rig was run for several hours with combustion chamber exit conditions up to 16 bar and 1500 K. The probe survived all the 167 injections (not counting no-flow trial runs), being immersed in the hot flow for up to 200 ms during each run.

The pressure signals (Figure 35) appear to be very noisy while the probe is exposed to the cooling flow within the shroud tube, due to the turbulent cooling flow surrounding the retracted probe. Spectra and autocorrelations have therefore been obtained for the signal while the probe was beyond the cooling flow (position sensor > 65 mm).

A number of features can be inferred from these results. (Figure 36) First, the signal clearly shows low frequency flapping (also detected by the temperature probe, see below) of the whole hot jet with a low frequency of order 35 Hz, very similar to that detected by the temperature probe.

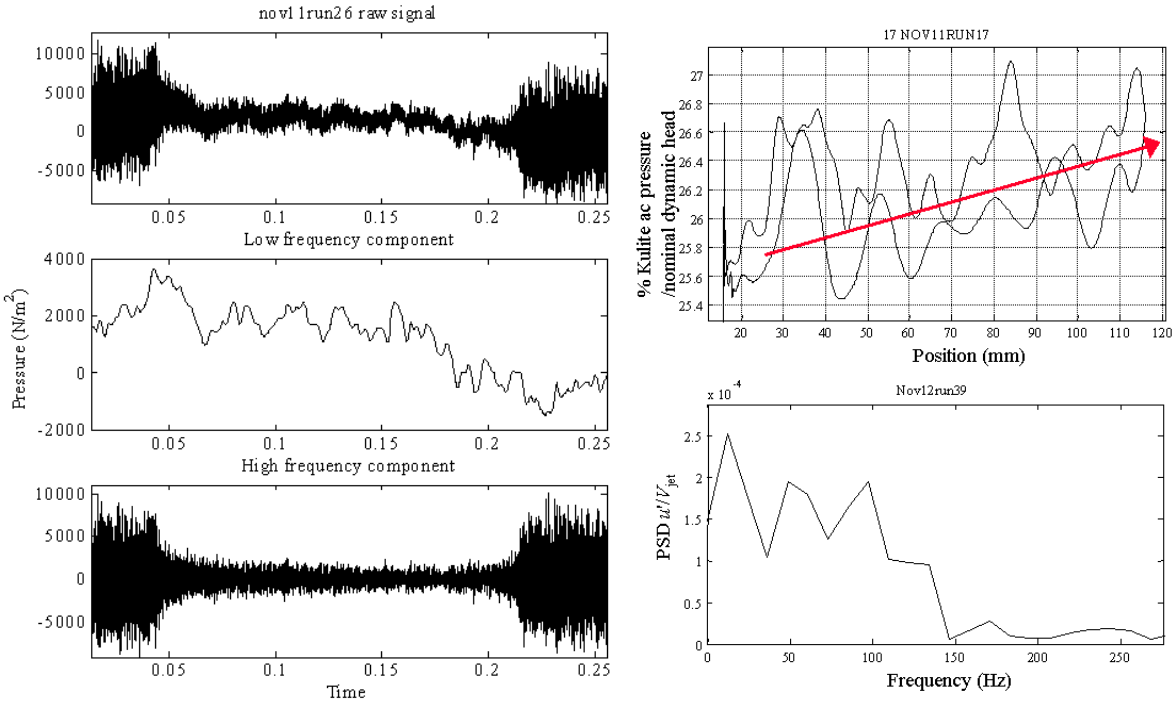

Figure 36 Low and high frequency components of the pressure signal, showing low frequency “flapping”, high frequency turbulence and the gradual rise in pressure as the probe enters the jet.

Underneath the flapping signature one can see the gradual rise in total pressure as the probe enters the jet; moreover some signals show a variety of low-frequency components to this flapping, so one must presume that the flapping characteristic is to some extent Reynolds number dependent.

The quality of the frequency spectra is improved by ensemble-averaging spectra from multiple tests. This is only sensible for tests at very similar conditions, for which similar spectra would be expected (and are indeed found); three test conditions, in terms of pressure and velocity, were therefore identified for this purpose. (Figure 37)

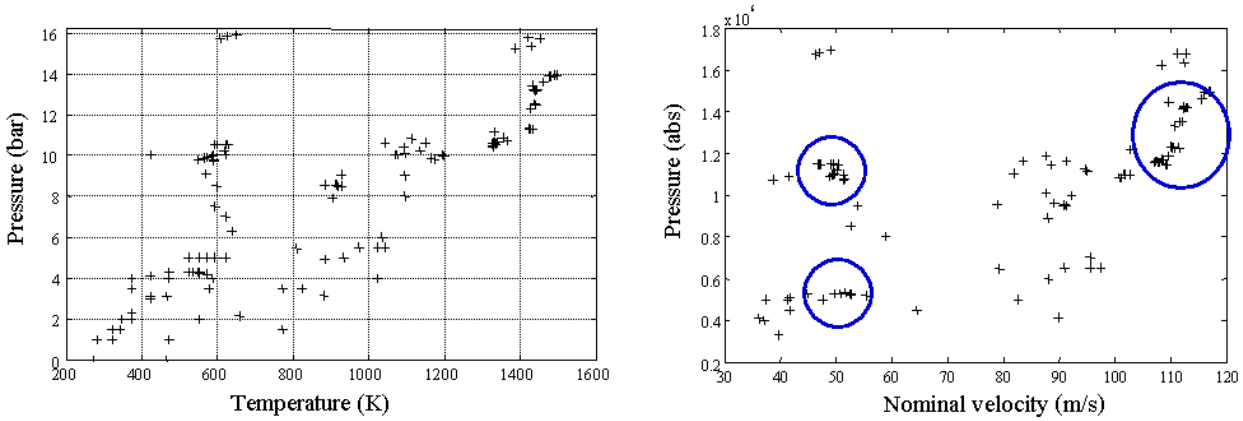

Figure 37 Choice of three nominal conditions: groups of runs sufficiently close in pressure, temperature and velocity to allow ensemble averaging of the spectra.

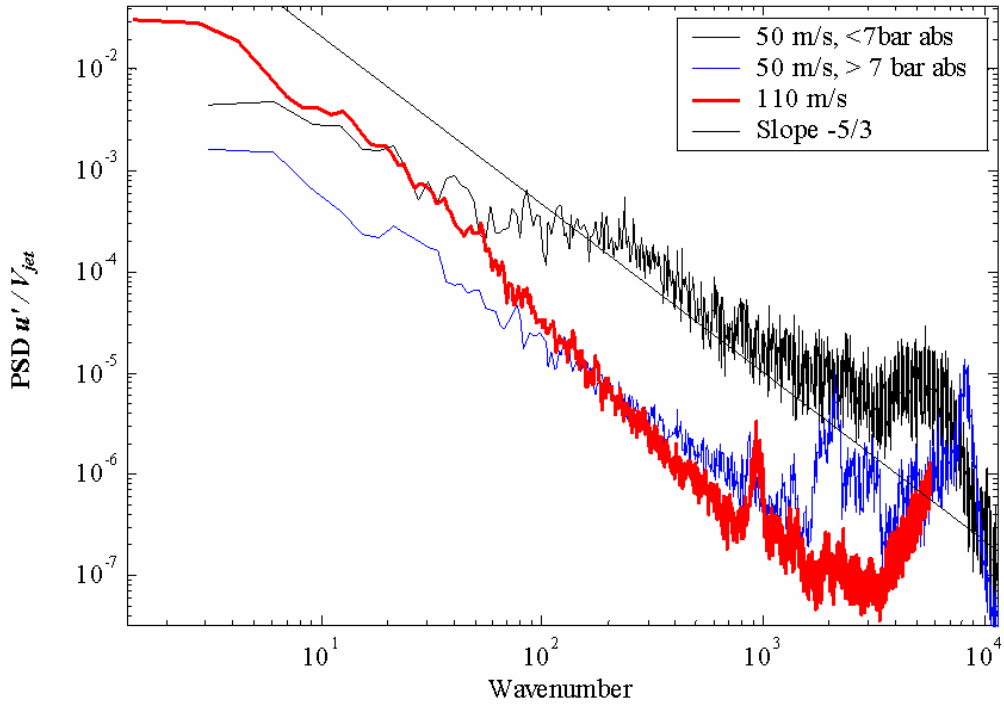

Figure 38 Ensemble-averaged spectra at three nominal conditions plotted against wavenumber.

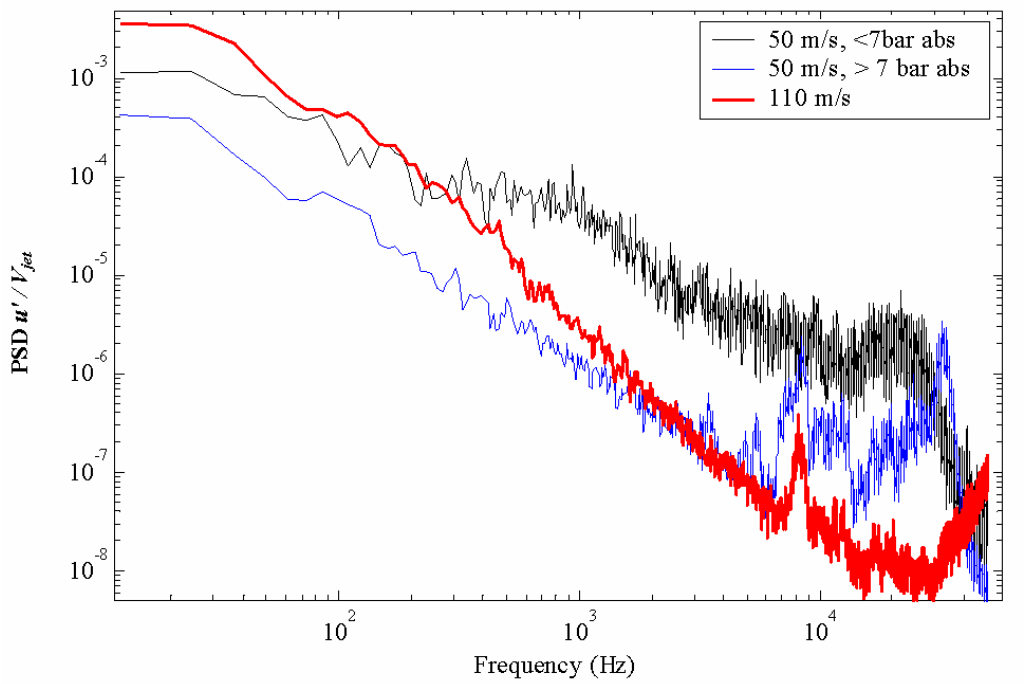

Figure 39 Ensemble-averaged spectra at three nominal conditions plotted against frequency. RMS fluctuation levels are 48%, 20% and 45% respectively. Some peaks occur at constant frequency rather than the expected constant wavenumber.

The different test conditions produce a variety of spectra which do not, overall, follow the classical turbulence spectra curve: this is almost certainly due to the very large low frequency fluctuations. (Figure 38, Figure 39)

The rms turbulence intensity is obtained by integrating the area under each spectrum. Comparing the three spectra, one finds that there are large variations in overall power. The high wavenumber components in each spectrum here all roll off with a –5/3 exponent that is characteristic of turbulence spectra. The differences in level, at high frequency, suggest that the low pressure flow (black) is rather different, in terms of flow features, than the two high pressure conditions. Whilst we have no in-depth explanation for this change, its existence is intriguing and demonstrates the value of having such an experimental technique for use at high pressures.

Some of the peaks in these spectra appear fixed in frequency rather than wavenumber and are thus presumably the result of a mechanical resonance or, possibly, an acoustic signal originating from a pre-combustor region of constant air temperature. One would expect any random flow feature such as vortex shedding to have a characteristic wavelength [Moss and Oldfield, 1991]; these peaks do not change frequency in the expected manner as the velocity changes.

Finally autocorrelations were calculated: most of them exhibit a sharp central spike due to random noise (possibly acoustic, see section 5.1). Autocorrelations are scaled to a peak value of 1: the spike, where present, affects the level of the rest of the curve (Figure 40 upper), so it has been removed and the correlation rescaled. (Figure 40 lower)

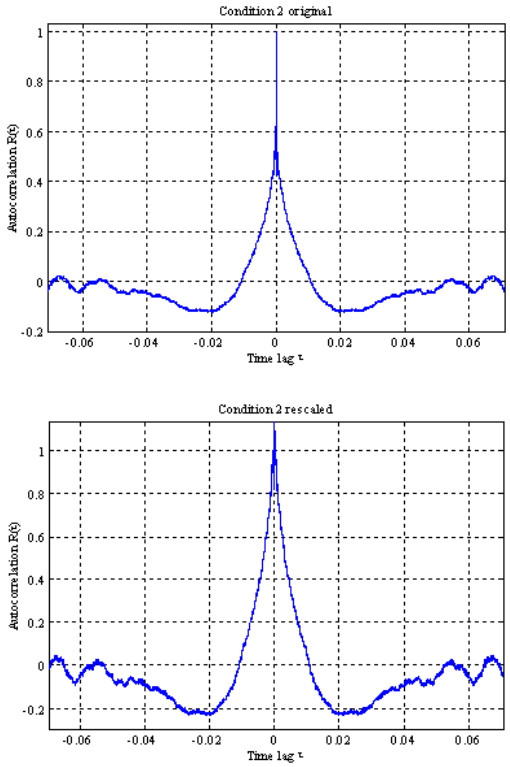

Figure 40 Rescaling of autocorrelations to avoid effect of central spike on length scales.

Integral length scales based on assumed jet velocity are typically 0.1m at the 50m/s condition and 0.3m at the 100m/s condition. The latter signal is dominated by the low frequency flapping signature and the length scale is really measuring this: it is not a *turbulence* length scale.

7.2 Temperature probe

The temperature probe hot test session was carried out in Sesta facility on 12 December 2002. The rig was run for 5 hours with conditions up to 16 bar and 1600 K for combustion chamber exit conditions. The probe survived 88 injections before being damaged by the flow, with immersion times in the hot flow up to 200 ms each run. (Figure 41)

Test Condition	Number of runs	Penetration Distance [mm]	ptot [bar]	Ttot [°C]	mdot [kg/s]
Cold 1	8	133.37	2.91	155	6.1
Hot 1	3	45.2	14.1	1260	22.6
Hot 2	5	32.8	15.4	1150	25.3
Hot 3	2	55.35	12.4	1060	20.6
Hot 4	7	33.5	11.2	1062	18.7
Hot 5	11	58.3	10.6	1010	18.5
Hot 6	11	68	9.88	916	18.5
Hot 7	7	101.2	8.58	897	18.3

Table 6 Summary of test condition for temperature probe

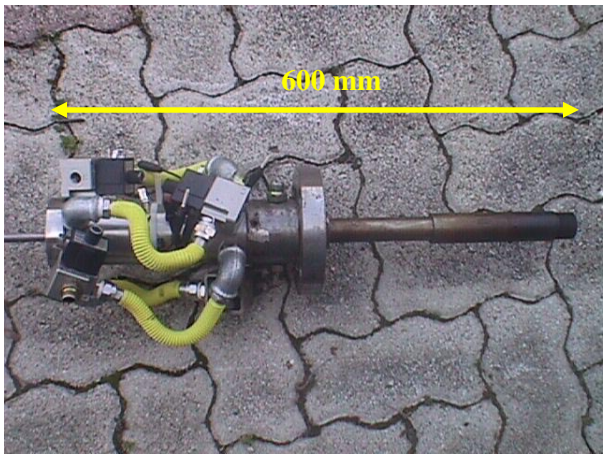

Figure 41 Injection mechanism after hot temperature tests.

The temperature probe was able to retrieve total temperature both in low and high temperature flows, and this revealed an important feature of the flow itself: the combustor exit flow, in the form of a jet through the centre of the instrumentation chamber, was flapping about due to some kind of low frequency instability. The probe head appeared to be periodically experiencing both the jet flow and the surrounding separation. The frequency was typically about 35 Hz, too big to be associated with jet shear layer eddies: this feature is particularly evident considering the probe heat flux for two runs, (Figure 42) the first before combustion chamber ignition and the second after ignition.

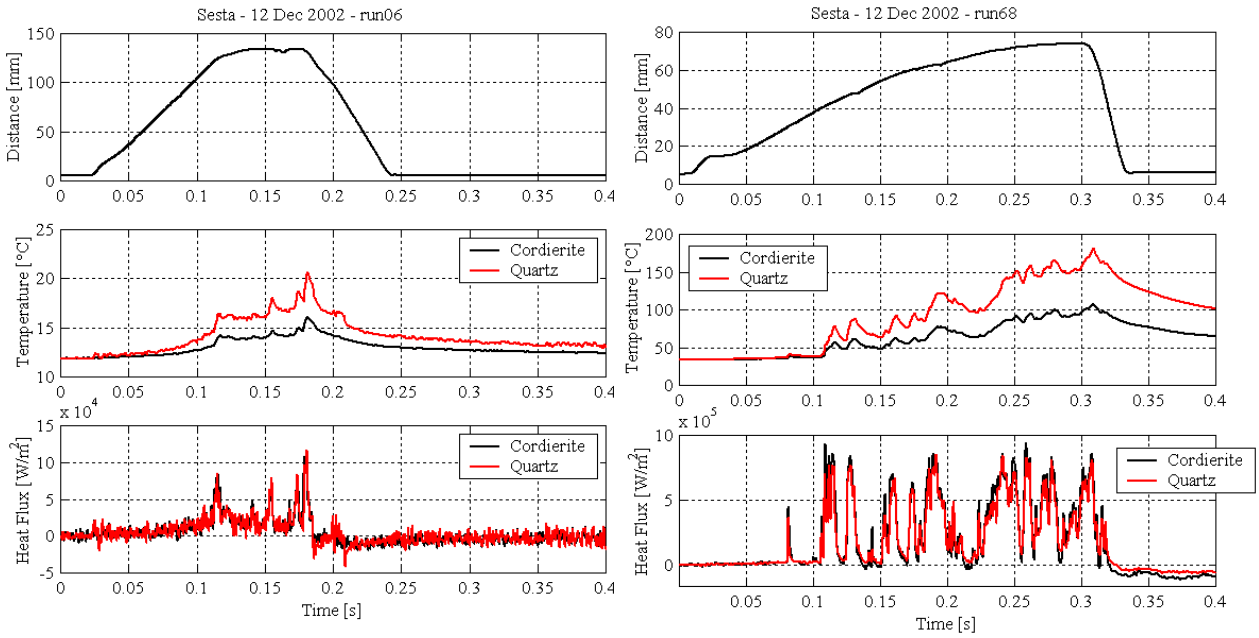

Figure 42 History of a cold run (left) and a hot run (right): when combustor is on, the probe appears to be alternately immersed in and out of the flow (heat flux oscillates between 0 and 800 kW/m^2 in the right figure).

The measured total temperature histories are consistent with the pressure probe results and are generally repeatable at a given test condition. They allowed the rig jet mean temperature profile (Figure 43, Figure 44) to be determined, and show that the nominal value (Figure 45) is obtained beyond about 70 mm of penetration and exhibits oscillations of about ±15%.

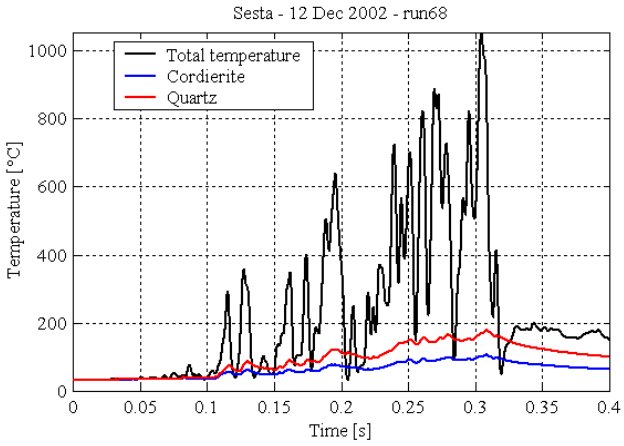

Figure 43 Typical total temperature history for a hot run.

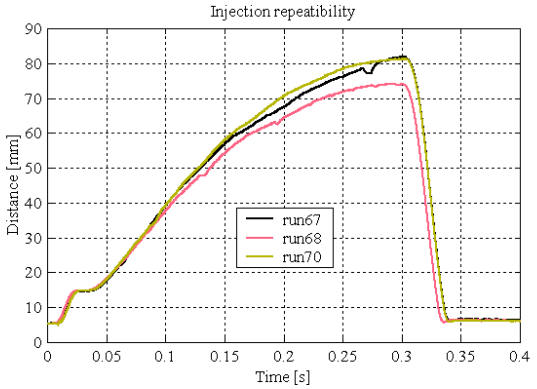

Figure 44 Repeatability of injection patterns for rig constant conditions.

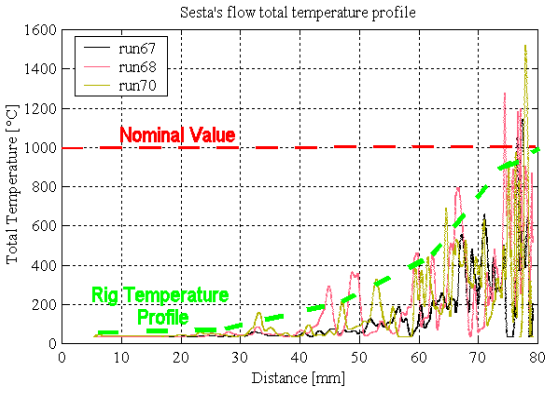

Figure 45 Retrieved rig jet mean temperature profile and fluctuations.

The results are consistent with calculations of convective heat flux on the stagnation point of a cylinder in cross-flow:

$$Nu = \frac{h \cdot D}{k} \cong \sqrt{\mathrm{Re}_D}$$
$$q_{dot} = h \cdot (T_{Tot} - T_{in})$$

Considering only data recorded by one of the films, and assuming to know mean flow properties, it is possible to develop an iterative procedure that allows to determine h and T_{tot}. Considering zones with an almost constant heat flux ten test points were considered (blue dots in Figure 46) and the temperatures retrieved via this method (red dots in Figure 46) compare consistently with the measured values (average error < 9%). The only point were results differ significantly is point 10 where relative error is 19% (see next table). This can be explained considering that point 10 happen to be located during probe retraction, which occurs much faster than probe insertion (probably due to coupling of motion with combustor back pressure) limiting post-processing accuracy.

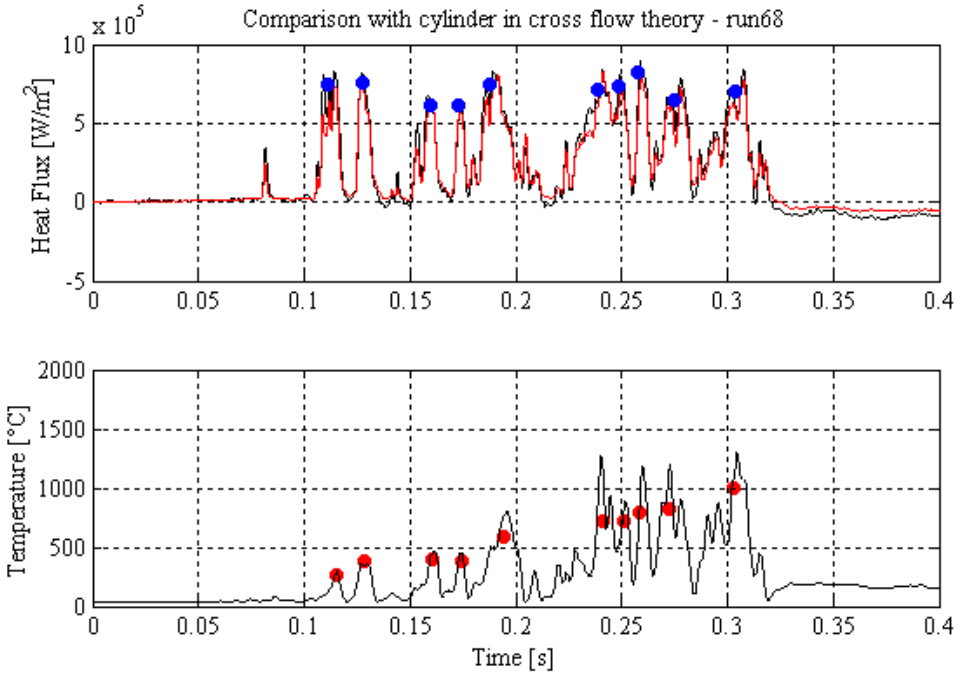

Figure 46 Comparison with cylindrical stagnation heat transfer theory: test points (up) – total temperature (down).

Point #	qdot/1e5 [W/m2]	T0q [°C]	Re/1e4 [-]	Nu [-]	Ttot-theory [°C]	Ttot-meas [°C]	% Error [-]
1	5.5	62	4.07	201.7	319	299	7
2	6.6	83	3.57	188.9	389	360	8
3	6.5	86	3.58	189.2	386	430	10
4	5.5	91	2.6	161.2	385	418	8
5	6.8	96	1.33	115.3	550	650	15
6	7.3	120	1.0	99.5	705	751	6
7	7.5	125	1.0	99.8	677	704	4
8	8.3	140	1.0	99.8	750	798	6
9	7.5	145	0.8	89.4	762	803	5
10	8.0	150	0.8	89.4	810	1002	19

Table 7 Comparison with cylindrical stagnation heat transfer theory: results for each test point

Minimum detectable temperature fluctuations are of order 5-10 K. Tests show that the self-heating two-substrate temperature probe has considerable promise although more work is needed on substrate calibration.

8. Future developments

Although the results of this work were very satisfactory, the practical experience gained from these tests led to several ideas for general improvement of the technique and its related devices.

- Improve design of injection/traverse mechanism:

– Modified design in order to include multiple sensors on a single probe
– More user-friendly (for quick probe replacement and test turnover)
– More flexible, for adaptation to different test rigs and to allow injector to operate on separate bottle air source

- Improve performance of pressure probe by reintroduction of low frequency total pressure measurement, temperature drift compensation, and also by inclusion of a separate transducer to act as a microphone and detect acoustic fluctuations.
- Improve understanding of temperature probe by characterization of high temperature material properties of different film substrates.

- Verification of above design changes with tests in the core flow near the exit plane of an operating combustor rig.

9. Conclusions

The experiments carried out in the hot, high pressure flow demonstrated the capability to take high bandwidth measurements in combustor environment using transient techniques: a portable fast injection device was designed and tested in real combustor with flow immersion time 100 to 200 ms.

Two probes were designed, manufactured and tested in order to retrieve pressure and temperature fluctuations: the pressure probe survived 167 runs with peak conditions of 16 bar (abs) and 1500 K, and the temperature probe successfully recorded data for over 80 injections with pressures up to 16 bar and temperatures up to 1600 K.

Very little electrical noise was recorded due to advanced amplifier design and portability of instrumentation was confirmed with probe installed and de-installed daily.

In particular, pressure flow measurements agree with the temperature probe conclusions: a large-scale flapping motion of the jet is the main unsteady phenomenon in this particular facility. This is large enough to mask the underlying turbulence. If measurements had been made close to combustor exit, then turbulence indications would be most likely successfully extracted.

The new self-heating two-substrate design chosen for the total temperature probe, although somewhat less sensitive than previous preheated probe, proved to be effective. Probe calibration and post-processing routines were confirmed by comparison with two other different methods for data reduction.

10. References

[1] Anderson, T.J. and Eckbreth A.C., 1992, "Simultaneous Coherent Anti-Stokes Raman Spectroscopy Measurements in Hydrogen-Fueled Supersonic Combustion", J. Propulsion and Power, Vol. 8, No. 1.

[2] Anthony, R.J., Oldfield, M.L.G., Jones, T.V., LaGraff, J.E., 1999, “Development of High-Density Arrays of Thin Film Heat Transfer Gauges”, Proceedings of the 5th ASME/JSME Thermal Engineering Joint Conference, San Diego, CA. AJTE99–6159.

[3] Battelle, R.T., 2001, "Design, Optimisation, and Testing of a Rapid Traversing Pressure Transducer for Measurement of Turbulent Spectra in a Gas Turbine Combustion Chamber", M.Sc. Thesis, Syracuse University.

[4] Biagioni, L. and d’Agostino, L., 1999, "Measurement of Energy Spectra in Weakly Compressible Turbulence", AIAA 99–3516, 30th Fluid Dynamics Conference, Norfolk, VA.

[5] Buttsworth, D.R. and Jones, T.V., 1996, "A Fast-Response Total Temperature Probe for Unsteady Compressible Flows", ASME Paper 96–GT–350.

[6] Buttsworth, D.R. and Jones, T.V., 1997a, "A Fast-Response High Spatial Resolution Temperature Probe Using a Pulsed Heating Technique", ASME Paper 97–GT–301.

[7] Buttsworth, D.R. and Jones, T.V., 1997b, "Radial Conduction Effects in Transient Heat Transfer Experiments", The Journal of the Royal Aeronautical Society, May 1997.

[8] Buttsworth, D.R. and Jones, T.V , Chana, K.S., 1997, "Unsteady Total Temperature Measurements downstream of a High Pressure Turbine", Journal of Turbomachinery 1998, vol 120, ASME Paper 97–GT–407.

[9] Dyne P.J. and Penner S.S., 1953, "Optical Methods for the Determination of Combustion Temperatures", ARS Journal, May–June 1953.
[10] Fagan J.R. and Fleeter S., 1994, "Comparison of Optical Measurement Techniques for Turbomachinery Flowfields", J. Propulsion and Power, Vol. 10, No. 2, pp. 176–182.
[11] Fiock E.F. and Dahl A.I., 1953, "The Measurement of Gas Temperature by Immersion-Type Instruments", ARS Journal, May–June 1953,pp.155–169.
[12] Gulati A., 1994, 'Raman Measurements at the Exit of a Combustor Sector", J. Propulsion and Power, Vol. 10, No. 2, pp. 169–175.
[13] Gulati A. and Warren R.E., 1994, "NO2-Based Laser-Induced Fluorescence Technique to Measure Cold-Flow Mixing", J. Propulsion and Power, Vol. 10, No. 1.
[14] Kerrebrock, 1992, "Aircraft Engines and Gas Turbines", Cambridge University Press, second edition.
[15] Klavuhn K.G., Gauba G. and McDaniel J.C, 1994, "OH Laser-Induced Fluorescence Velocimetry Technique for Steady High-Speed, Reacting Flows", J. Propulsion and Power, Vol.10, No.6, pp.787–797.
[16] Moss, R.W., and Oldfield, M.L.G., 1990, Comparisons between Turbulence Spectra Measured with Fast Response Pressure Transducers and Hot Wires. Symposium on Aerodynamic Measuring Techniques for Transonic and Supersonic Flow in Cascades and Turbomachines, VKI
[17] Moss, R.W. and Oldfield, M.L.G., 1991, "Measurements of Hot Combustor Spectra", ASME IGTI 1991 Gas Turbine Conference, Orlando, ASME91–GT–351.
[18] Moss, R.W. and Oldfield, M.L.G., 1992, "Measurements of the Effect of free-Stream Turbulence Length Scale on Heat Transfer", ASME IGTI 1992 Gas Turbine Conference, Cologne, ASME 92–GT–244.
[19] Moss, R.W. and Oldfield, M.L.G., 1996, "Effect of Free-stream turbulence on Flat-plate Heat Flux signals: Spectra and Eddy Transport Velocities", ASME Journal of Turbomachinery, Vol. 118, pp. 461–467 (Also ASME Paper 94–GT–205).
[20] Ng W.F. and Epstein A.H., 1983, "High-Frequency Temperature and Pressure Probe for Unsteady Compressible Flows" Rev. Sci. Instrum., Vol. 54, No. 12, pp. 1658–1683.
[21] Oldfield, M.L.G., 2000,“Guide to Impulse Response Heat Transfer Signal Processing Version 2.”, Oxford University Engineering Laboratory OUEL Report 2233/2000, 1 October 2000.
[22] Pondicq-Cassou, N., 2001, "Design of a Cooling System Adapted to a Fast Injection Device", Projet de fin d’Etudes (Final year thesis), ENSICA, Toulouse, France.
[23] Torre, S, 1999, "Development of a Fast Injection Device for the Measurement of Turbulent Flow", Tesi di Laurea, Centrospazio, Università degli Studi di Pisa, Pisa, Italy.

REPORT DOCUMENTATION PAGE

Form Approved
OMB No. 0704-0188

1. AGENCY USE ONLY (*Leave blank*)	2. REPORT DATE	3. REPORT TYPE AND DATES COVERED
	September 2003	Final Contractor Report

4. TITLE AND SUBTITLE

Measurement of Turbulent Pressure and Temperature Fluctuations in a Gas Turbine Combustor

5. FUNDING NUMBERS

WBS–22–710–10–01
NAG3–2419

6. AUTHOR(S)

Andrea Passaro, John E. LaGraff, Martin L.G. Oldfield, Leonardo Biagioni, Roger W. Moss, and Ryan T. Battelle

7. PERFORMING ORGANIZATION NAME(S) AND ADDRESS(ES)

Syracuse University
100 University Place
Syracuse, New York 13244

8. PERFORMING ORGANIZATION REPORT NUMBER

E–14106

9. SPONSORING/MONITORING AGENCY NAME(S) AND ADDRESS(ES)

National Aeronautics and Space Administration
Washington, DC 20546–0001

10. SPONSORING/MONITORING AGENCY REPORT NUMBER

NASA CR—2003-212540

11. SUPPLEMENTARY NOTES

Andrea Passaro and Leonardo Biagioni, Centrospazio–CPR, Pisa, Italy; John E. LaGraff and Ryan T. Battelle, Syracuse University, 100 University Place, Syracuse, New York 13244; Martin L.G. Oldfield, University of Oxford, Oxford, United Kingdom; Roger W. Moss, University of Newcastle upon Tyne, Newcastle upon Tyne, United Kingdom. Project Manager, Louis A. Povinelli, Research and Technology Directorate, NASA Glenn Research Center, organization code 5000, 216–433–5818.

12a. DISTRIBUTION/AVAILABILITY STATEMENT

Unclassified - Unlimited
Subject Category: 07 Distribution: Nonstandard

Available electronically at http://gltrs.grc.nasa.gov

This publication is available from the NASA Center for AeroSpace Information, 301–621–0390.

12b. DISTRIBUTION CODE

13. ABSTRACT ***(Maximum 200 words)***

The present research concerns the development of high-frequency pressure and temperature probes and related instrumentation capable of performing spectral characterization of unsteady pressure and temperature fluctuations over the 0.05–20 kHz range, at the exit of a gas turbine combustor operating at conditions close to nominal ones for large power generation turbomachinery. The probes used a transient technique pioneered at Oxford University; in order to withstand exposure to the harsh environment the probes were fitted on a rapid injection and cooling system jointly developed by Centrospazio–CPR and Syracuse University. The experimental runs were performed on a large industrial test rig being operated by ENEL Produzione. The achieved results clearly show the satisfactory performance provided by this diagnostic tool, even though the poor location of the injection port prevented the tests from yielding more insight of the core flow turbulence characteristics. The pressure and temperature probes survived several dozen injections in the combustor hot jet, while consistently providing the intended high frequency performance. The apparatus was kept connected to the combustor during long duration firings, operating as an unobtrusive, self contained, piggy-back experiment: high frequency flow samplings were remotely recorded at selected moments corresponding to different combustor operating conditions.

14. SUBJECT TERMS

Gas turbine fluctuations; Turbulence spectra in combustors; Pressure and temperature spectra; Gas turbine combustors; Unsteady flow; Turbulence; Hot flow sensors

15. NUMBER OF PAGES

30

16. PRICE CODE

17. SECURITY CLASSIFICATION OF REPORT	18. SECURITY CLASSIFICATION OF THIS PAGE	19. SECURITY CLASSIFICATION OF ABSTRACT	20. LIMITATION OF ABSTRACT
Unclassified	Unclassified	Unclassified	